NANOPARTICLES ENGINEERED TO BIND SERUM ALBUMIN: MICROWAVE ASSISTED SYNTHESIS, CHARACTERIZATION, AND FUNCTIONALIZATION OF FLUORESCENTLY-LABELED, ACRYLATE-BASED, POLYMER NANOPARTICLES

Barbara R. Hinojosa, B.S.

Thesis Prepared for the Degree of

MASTER OF SCIENCE

UNIVERSITY OF NORTH TEXAS

August 2010

APPROVED:

Robby A. Petros, Major Professor
Weston T. Borden, Committee Member
William E. Acree Jr., Chair of the Department of Chemistry
James D. Meernik, Acting Dean of the Robert B. Toulouse School of Graduate Studies

Hinojosa, Barbara R. Nanoparticles engineered to bind serum albumin: Microwave assisted synthesis, characterization, and functionalization of fluorescently-labeled, acrylate-based, polymer nanoparticles. Master of Science (Chemistry-Organic Chemistry), August 2010, 69 pp., 11 tables, 21 illustrations, bibliography, 49 titles.

The potential use of polymeric, functionalized nanoparticles (NPs) as drug delivery vectors was explored. Covalent conjugation of albumin to the surface of NPs via maleimide chemistry proved problematic. However, microwave assisted synthesis of NPs was not only time efficient, but enabled the exploration of size control by changing the following parameters: temperature, microwave power, reaction time, initiator concentration, and percentage of monomer used. About 1.5 g of fluorescently-labeled, carboxylic acid-functionalized NPs (100 nm diameter) were synthesized for a total cost of less than $1. Future work will address further functionalization of the NPs for the coupling of albumin (or other targeted proteins), and tests for in vivo biodistribution.

TABLE OF CONTENTS

Page

LIST OF TABLES

Page

LIST OF ILLUSTRATIONS

Page

CHAPTER 1

INTRODUCTION

The objective of this introductory chapter is to present the reader with some basic background information that will help in the understanding of the purpose of this research. The problems associated with drug delivery have sparked an interest in developing a better delivery system that will result in a better prognosis for the patient receiving treatment. Thus the objective of this work was to synthesize nanoparticles (NPs) as a drug delivery vector, functionalize the surface of NPs, and test their biodistribution. Initial work focused on the functionalization of commercially available nanoparticles; however, it quickly became clear that in order to fully investigate the effects of nanoparticle surface coatings on biological properties, the ability to synthesize nanoparticles from inexpensive starting materials was needed. This chapter briefly discusses the major problems of drug delivery, and the current delivery vectors designed to overcome these issues. Since the basis of this research was the potential use of albumin-coated delivery vectors, a section defining the properties of albumin is also included. Chapter 2 focuses on the preliminary experimental work conducted in an effort to couple albumin onto commercially available amine-terminated NPs. The motivation behind this work was to observe how NPs function in vivo, and hopefully gain a better understanding of

how to control in vivo properties via selective surface coatings. Chapter 3 deals with the synthesis of fluorescently-labeled, acrylate-based NPs through microwave-assisted, thermal initiation of free-radical polymerization reactions. This chapter starts off with a brief description of different methods currently used to synthesize NPs, followed by the experimental work and discussion of results. Finally, Chapter 4 discusses future work that will be completed by other members of this group in order to make a full evaluation on the NPs synthesized and their potential use as drug delivery vectors. This future work refers to further functionalization of the NPs for the coupling of albumin (or other targeted proteins), and tests for in vivo biodistribution.

1.1 Barriers to Targeted Drug Delivery

The vast majority of potential therapeutic drugs have poor pharmacokinetics and biopharmaceutical properties. [1] Problems commonly encountered in many drugs include: insufficient stability (shelf life), short in vivo stability (half life), poor solubility, low bioavailability, and toxicity to non-target tissues. A solution to these problems is the incorporation of the drug into a particulate carrier which can protect it against degradation, can control the release of drug, and offer possibilities for targeting the drug to selected cells or tissues.[2] Although, nanodelivery systems have shown potential as drug carriers by combining tissue/organ-specific targeting with therapeutic action, premature removal from circulation via phagocytosis continues to be an important biological obstacle to controlled drug delivery. Phagocytosis is the removal of

nanoparticulate drug carriers from the body by the reticuloendothelial system (RES). When nanocarriers that are larger than ~200 nm, or many foreign substances, enter blood circulation opsonin proteins adsorb to their surface, forming a “protein-corona”, and render the nanocarrier more visible to macrophages. Macrophages of the spleen and liver, the latter also known as Kupffer cells, recognize the “protein-corona” and begin the process of phagocytosis- leading to premature clearance from blood circulation.[3, 4] Preventing phagocytosis of the nanocarriers, and thus increasing circulation time, is a current focus of research in the Petro’s lab, and is necessary for successful targeted drug delivery.

1.2 Targeted Drug Delivery Vectors

The requirements of designing a successful drug delivery system are the following: improvement of drug stability and absorption, to permit reproducible and long-term release of the drug at the target site, and increasing therapeutic concentration of the drug within the target tissue. The advancement of nanotechnology has been implemented for developing drug delivery vectors that meet these requirements. [5] The following sections of this chapter will briefly describe the current nanoscale drug delivery systems, which include: liposomes, micelles, nanoemulsions, dendrimers, and nanoparticulate systems.

1.2.1 Liposomes

Liposome technology was discovered over 40 years ago, they are small artificial vesicles of spherical shape that can be produced from natural nontoxic

phospholipids and cholesterol (see Figure 1) [6]. They are particularly useful in serving as drug-carriers for nanodelivery systems due to their ability to pass through lipid bilayers and cell membranes.[5] Although liposomes vary greatly in size, ones used for drug delivery are usually 400 nm or less in diameter to avoid clearance from blood circulation. Liposomes can be classified in terms of composition and mechanism of intracellular delivery into five types: conventional liposomes, pH-sensitive liposomes, cationic liposomes, immunoliposomes, and long-circulating liposomes. Researchers have studied a range of surface modifications that can be made to conventional liposomes to increase their circulation half-lives for effective targeting. These modifications include incorporation of linear dextrans, sialic acid-containing gangliosides, and lipid derivatives of hydrophilic polymers such as poly(ethylene-glycol) PEG , poly-N-vinylpyrrolidones and polyvinyl alcohol, to provide steric stabilization around the liposomes for protection from uptake via the RES.[5] Although there are a number of liposome-based drug formulations available, many have not entered the market due to the following problems: liposome stability, poor batch-to-batch reproducibility, difficulties in sterilization, and low drug loading.[5, 7, 8]

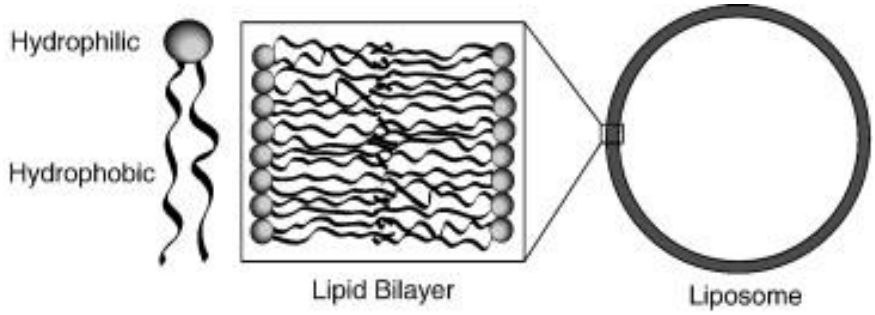

Figure 1. Schematic Diagram of a Liposome[6]

1.2.2 Micelles

Micelles are self-assemblies of amphiphiles that form supramolecular core-shell structures in an aqueous medium (see Figure 2) [7]. These systems are composed of amphiphilic polymers that consist of polyethylene glycol (PEG) and a low-molecular-weight hydrophobic core-forming block. [5] Micelles are useful for increasing the solubility of poorly water-soluble drugs, such as anticancer agents, by incorporating them into their hydrophobic core. They are generally smaller than 100 nm, which provides an advantage over liposomes-typically 100-400 nm in diameter. Due to their small size and hydrophilic surfaces, micelles can evade host defenses, thereby increasing their blood circulation time. Micellar drug delivery systems can be divided into the following classes: phospholipid micelles, pluronic micelles, poly (L-amino acid) micelles, and polyester micelles. It has been found that the encapsulation of doxorubicin (DXR), Cis-platin, and paclitaxel in micelles increases their circulation half-life and tumor accumulation. [5, 7, 9]

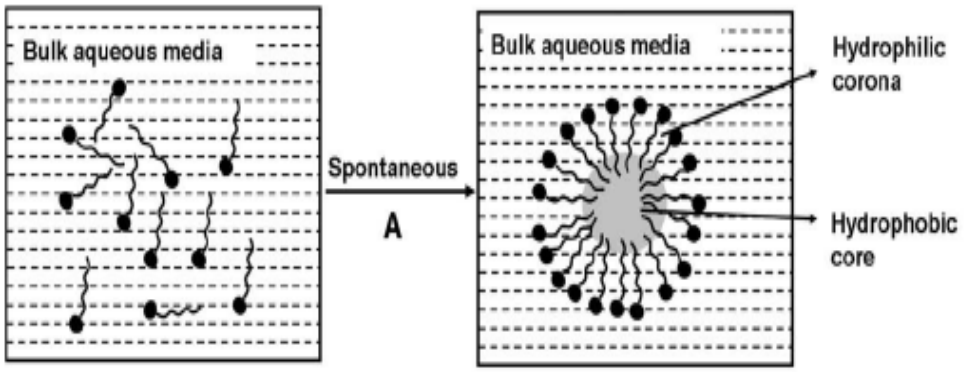

Figure 2. Diagram of Micelles: Formation of Micelles in Aqueous Media [7]

1.2.3 Nanoemulsions

Nanoemulsions are dispersions of oil and water where the dispersed phase droplets are stabilized with a surface active film composed of surfactant and co-surfactant. They are transparent systems that have a dispersed-phase droplet size range of typically 20 to 200 nm. Nanoemulsions containing >50 wt% water are considered oil-in-water (O/W), and those containing <20 wt% water are water-in-oil (W/O) nanoemulsions. In an O/W nanoemulsion, hydrophobic drugs are solubilized mainly in the oil droplets and will be released slowly due to hindered diffusion, while the diffusion of hydrophilic drugs is less restrained and they will be released quickly; and the reverse is expected in a W/O nanoemulsion.[5] The attraction of nanoemulsions is due to the following advantages: (i) the small droplet size helps prevent sedimentation from occurring on storage, (ii) the small droplet size also prevents any flocculation of the droplets and this enables the system to remain dispersed with no separation, (iii) nanoemulsions are suitable for efficient delivery of active ingredients through

the skin, (iv) the small size of the droplets allows them to deposit uniformly on substrates, (v) lastly, nanoemulsions are much more stable than liposomes. Despite these advantages, comparatively little research is being conducted in this area because of to the high cost of production, as well as the lack of understanding of the interfacial chemistry that is involved in their production. [10]

1.2.4 Dendrimers

Dendrimers are a unique class of macromolecules synthesized by a series of controlled reactions. They are characterized by multiple branching around the central core, which provide multiple functional groups on their surface (see Figure 3) [7]. The polyvalent nature of a dendrimer allows it to activate many receptors simultaneously, whereas a small molecule can only interact with one receptor. Functional groups such as carbohydrates, peptides, and silicon can be used to form glycodendrimers, peptide dendrimers, and silicon-based dendrimers, respectively. [11] Their typical size of 10 to 100 nm renders them ideal for targeted drug delivery. Dendrimer drug-delivery systems that have been proposed include: encapsulation of drug molecules in the void spaces of the dendrimer interior, dendrimer-drug networks, and linking therapeutic agents to the surface of dendrimers as prodrugs. Pharmaceutical applications of dendrimers include the following: nonsteroidal anti-inflammatory formulations, antimicrobial and antiviral drugs, anticancer agents, pro-drugs, and screening agents for high-throughput drug discovery. [5, 7, 11]

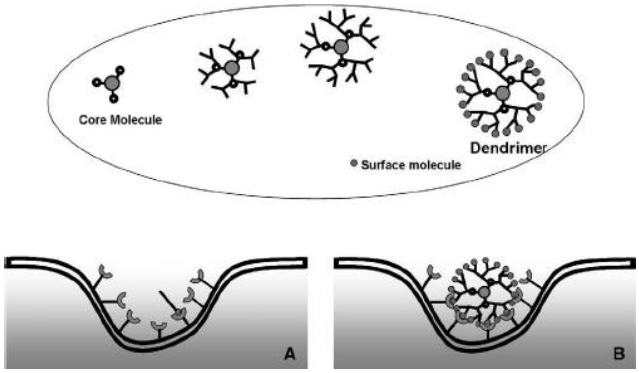

Figure 3. Dendrimer's Receptor Interaction
A. Small molecules can only interact with one receptor. In contrast, **B**. Dendrimers can interact with multiple receptors simultaneously.[7]

1.2.5 Nanoparticulate Systems

Nanoparticulate systems investigated for drug delivery include drug nanoparticles (DNPs), and solid nanoparticles (SNPs) - which are further classified into: polymer-based NPs, lipid-based NPs, ceramic-based NPs, and albumin NPs. DNPs are formed by breaking down bigger particles to nanosize using high-pressure homogenization in the presence of surfactants, or crystallization building from the supersaturated solution state of the drug. These types of NPs are attractive for the delivery of drugs that are not soluble in water or nonpolar solvents, and cannot be formulated by other methods. Polymer-based NPs are often made from copolymers containing PEG to increase circulation half-life and reduce RES uptake and inactivation. Poly(lactic acid) (PLA), poly(glycolic acid) (PGA), poly-*ε*-caprolactone, and poly(methyl methacrylate) (PMMA) are the most commonly used polymers due to their biocompatibility.[5] The PEGylation of NPs has been frequently used as an effective approach to depress the nonspecific binding of NPs to serum proteins

and macrophages, thereby bypassing hepatic clearance; this is called "stealthing" of NPs. The 'stealth' characteristics of PEGylated NPs are thought to result from the steric hindrance and repulsion effects of PEG chains against blood proteins and macrophages, which are closely correlated to the PEG molecular weight, surface chain density and conformation. The different conformations and molecular weights of PEG chains would directly affect their flexibility and hydrophilicity, respectively, and consequently their steric repulsion against blood proteins and macrophages.[12-16]Lipid based NPs have attracted significant interest by various researchers since the mid 1990s as an innovative drug delivery carrier system, because of their physical stability, protection of incorporated drugs from degradation, controlled release, and excellent tolerability.[7, 17] Ceramic- based NPs are made of biocompatible materials such as silica, alumina, and titania. Their preparations are not only simple, but also result in NPs with desirable size, shape, porosity, and inertness. [5] Albumin-based NPs are able to avoid opsonization and uptake by RES, because albumin protein is a major component of blood plasma. These NPs can be prepared by a desolvation/cross-linking technique, where an aqueous solution of albumin is desolvated by dropwise addition of ethanol and glutaraldehyde to induce albumin nanoparticle cross-linking over time. A major breakthrough in January 2005 was the FDA approval of the use of paclitaxel albumin NPs (~130 nm in size) for the treatment of metastatic breast cancer. [5, 18]

1.3 Albumin

Albumin is the most abundant plasma protein (35–50 g/L human serum) with a molecular weight of 66.5 kDa. Human serum albumin (HSA) consists of 585 amino acids containing 35 cysteine residues which build 17 disulfide bridges, however, one free thiol group, namely cysteine-34 (Cys-34), remains unbound.[18,19] Figure 4 shows the three-dimensional structure of HSA which has been elucidated by X-ray structure analysis.[20] The functions and binding properties of HSA are many: (i) it is essential for the metabolism of lipids; (ii) it binds bilirubin, the breakdown product of heme; (iii) it binds a great number of therapeutic drugs such as penicillins, sulfonamides, indole compounds, and benzodiazepines; (iv) it binds copper(II) and nickel(II) in a specific manner and calcium(II) and zinc(II) in a relatively nonspecific manner and acts as the transport vehicle for these metal ions in the blood; (v) it is the major protein responsible for the colloid osmotic pressure of the blood; (vi) and when HSA is broken down the amino acids provide nutrition to peripheral tissue. Based on these properties it is evident that HSA plays a key role in keeping our bodies functioning properly. Other essential characteristics of albumin include its stability in the pH range of 4–9, solubility in 40% ethanol, and being able to withstand temperatures of 60 °C for up to 10 h without denaturing. Studies have also shown that HSA has preferential uptake in tumor and inflamed tissue, ready availability and biodegradability, and its lack of toxicity and immunogenicity make it an ideal candidate for drug delivery.[19] Therefore researchers are now

focused on studying the effects of binding albumin to the surface of drug delivery vectors.[18,19]

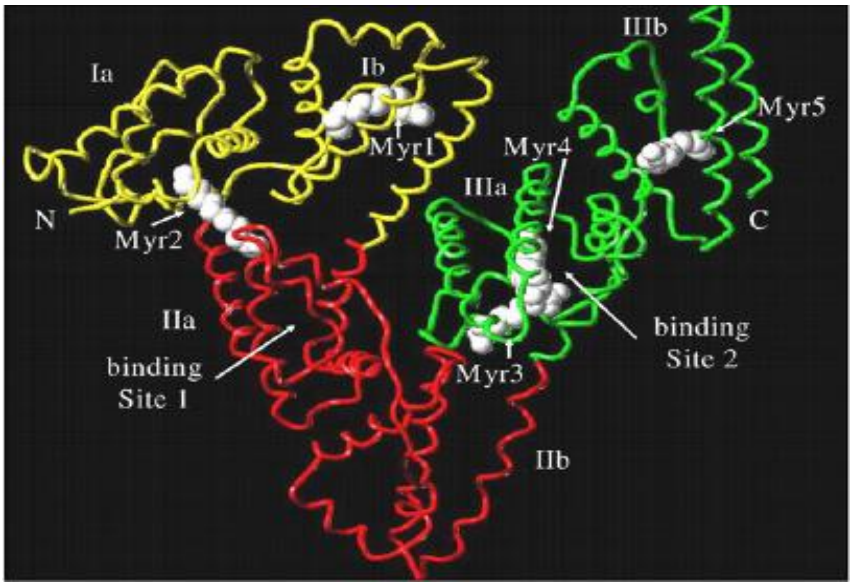

Figure 4. X-ray Structure of HSA [20]

1.4 Chapter References

1. Sahoo, S. K.; Parveen, S.; Panda, J. J. *Nanomedicine: Nanotechnology, Biology and Medicine* **2007,** *3,* 20-31.

2. Muller, R. H.; Keck, C. M. *J. Biotechnol.* **2004,** *113,* 151-170.

3. Owens III,D. E.; Peppas, N. A. *Int. J. Pharm.* **2006,** *307,* 93-102.

4. Aggarwal, P.; Hall, J. B.; McLeland, C. B.; Dobrovolskaia, M. A.; McNeil, S. E. *Adv. Drug Deliv. Rev.* **2009,** *61,* 428-437.

5. Koo, O. M.; Rubinstein, I.; Onyuksel, H. *Nanomedicine: Nanotechnology, Biology and Medicine* **2005,** *1,* 193-212.

6. Huang, S. *Adv. Drug Deliv. Rev.* **2008,** *60,* 1167-1176.

7. Bawarski, W. E.; Chidlowsky, E.; Bharali, D. J.; Mousa, S. A. *Nanomedicine: Nanotechnology, Biology and Medicine* **2008,** *4,* 273-282.

8. Zhang, J. A.; Anyarambhatla, G.; Ma, L.; Ugwu, S.; Xuan, T.; Sardone, T.; Ahmad, I. *European Journal of Pharmaceutics and Biopharmaceutics* **2005,** *59,* 177-187.

9. Lukyanov, A. N.; Torchilin, V. P. *Adv. Drug Deliv. Rev.* **2004,** *56,* 1273-1289.

10. Tadros, T.; Izquierdo, P.; Esquena, J.; Solans, C. *Adv. Colloid Interface Sci.* **2004,** *108-109,* 303-318.

11. Cloninger, M. J. *Curr. Opin. Chem. Biol.* **2002,** *6,* 742-748.

12. He, Q.; Zhang, J.; Shi, J.; Zhu, Z.; Zhang, L.; Bu, W.; Guo, L.; Chen, Y. *Biomaterials* **2010,** *31,* 1085-1092.

13. Francesco, M.V.; Gianfranco, P. *Drug Discov. Today* **2005,** *10,* 1451–1458.

14. Hamidi, M.; Azadi, A.; Rafiei, P. *Drug Deliv.* **2006,** *13,* 399–409.

15. Harper, G.R.; Davies, M.C.; Davis, S.S.; Tadros, T.F.; Taylor, D.C.; Irving, M.P. *Biomaterials* **1991,** *12,* 695–704.

16. Claesson, P.M.; Blomberg, E.; Froberg, J.C.; Nylander, T.; Arnebrant, T. *Adv. Colloid Interface Sci.* **1995,** *57,* 161–227.

17. Yang, S. C.; Lu, L. F.; Cai, Y.; Zhu, J. B.; Liang, B. W.; Yang, C. Z. *J. Controlled Release* **1999,** *59,* 299-307.

18. Langer, K.; Anhorn, M. G.; Steinhauser, I.; Dreis, S.; Celebi, D.; Schrickel, N.; Faust; S., Vogel, V. *Int. J. Pharm.* **2008,** *347,* 109-117.

19. Kratz, F., *J. Controlled Release* **2008,** *132,* 171-183.

20. Carter, D.C.; Ho, J.X. *Adv. Protein Chem.* **1994,** *45,* 153–203.

CHAPTER 2

BINDING OF SERUM ALBUMIN TO AMINE-TERMINATED NANOPARTICLES

2.1 Introduction

Several studies on the effect of coupling albumin onto the surface of delivery vectors agree that circulation time of these vectors in significantly increased.[1,2] The in vivo disposition of rat serum albumin-modified polyethylene-glycol (RSA/PEG) liposome was compared to that of the unmodified PEG-liposome. It was found that the hepatic clearance for RSA/PEG liposome was considerably smaller than that for PEG liposome. SDS-polyacrylamide gel electrophoresis (SDS-PAGE) was performed to analyze the amount of serum proteins (i.e. opsonins) that associated with the liposomes. The results revealed that less serum proteins bound to the surface of RSA/PEG liposome, which correlates with the decrease in hepatic clearance. [1] The same authors observed improved pharmacokinetic and pharmacodynamic properties of albumin-coated liposomes containing doxorubicin, DXR (see Figure 5).[2] DXR is an anthracycline drug used in the treatment of leukemia and lymphoma. However, there are many dose-related toxic side-effects, such as cardiotoxicity, which limit the clinical application of DXR. The observations of this study were decreased accumulation

of DXR in the liver, spleen and heart, an increased accumulation in the tumor, and an overall two-fold increase in therapeutic index of the drug. [3]

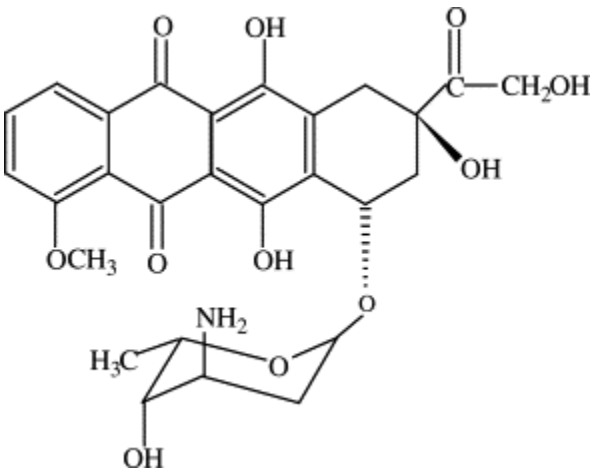

Figure 5. Chemical Structure of Doxorubicin [2]

Another group of researchers found similar results when they evaluated the in vivo disposition of polystyrene nanospheres (NS) with the particles size of 50 nm (NS-50). They pre-coated NS-50 with recombinant human serum albumin (rHSA), and observed that only one-ninth of the serum proteins that associated with uncoated NS-50 bound to the rHSA-coated NS-50. This resulted in less affinity to macrophages and prolonged circulation of the rHSA-coated NS-50.[4] Surface hydrophobicity of NS-50 has been shown to be the major determinant for its hepatic disposition.[5] Thus pre-coating NS-50 with rHSA, which is relatively hydrophilic, decreases the surface hydrophobicity of NS-50 and suppress its hepatic disposition.[4, 5]

As mentioned above, albumin is the most abundant protein in blood plasma and it also preferentially accumulates in solid tumors due to the high

metabolic turnover of tumor tissue and the enhanced vascular permeability for circulating macromolecules. Hence the coupling of albumin to anti-tumor drugs is a promising strategy for targeted drug delivery. [6, 7] About 70% of serum albumin is mercaptalbumin, which contains the accessible Cys-34. Furthermore, the free thiol group found at the Cys-34 position of serum albumin accounts for 80-90% of the thiol concentration in blood plasma. It is the high relative abundance and strong reactivity of the free thiol group in Cys-34 of albumin that makes it a good candidate for coupling to other molecules or macromolecules. The X-ray structure shows the position of cysteine-34 located in a hydrophobic crevice on the surface of albumin (See Figure 4). In order to open up this crevice and expose the thiol group of Cys-34, albumin is complexed to long-chain fatty acids such myristic acid (see Figure 6.)[7]

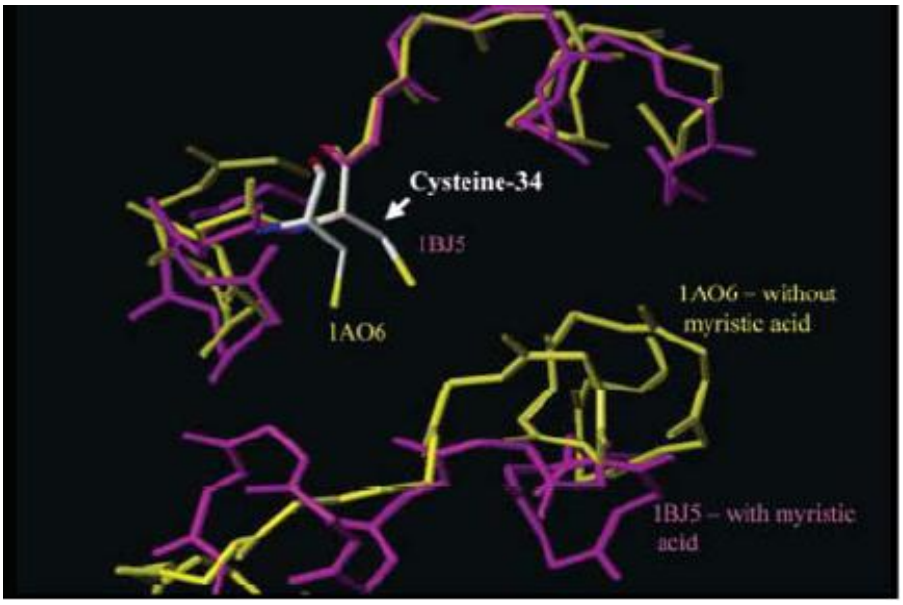

Figure 6. Three-dimensional Structure of the Cys-34: Binding Pocket of HSA and the Albumin Structure in which Five Molecules of Myristic Acid are Bound [7]

Methods have been proposed to bind drugs to albumin either endogenously or exogenously. Work done by Kratz and co-workers sought the use of albumin as an endogenous drug carrier by proposing a macromolecular prodrug strategy. This mechanism was based on: in situ binding of a thiol binding prodrug to the Cys-34 position of circulating albumin after intravenous administration, and release of the drug at the tumor site due to incorporation of an acid-sensitive bond between the drug and carrier.[7, 8] Doxorubicin derivatives **1-5** (see Figure 7) were synthesized, and their respective rate constants for binding to the Cys-34 were measured.[6] Molecular modeling of the covalent interaction of **3** with myristic acid bound albumin suggested that the optimal length of the polymethylene spacer is that of five carbons. The polymethylene spacer will interact with the hydrophobic channel of Cys-34, and the hydrophilic moieties of **3** interact with polar amino acids at the opening of the channel. For endogenous binding, **3** was incubated with human blood plasma at 37 °C, and analysis by reverse-phase chromatography revealed that coupling of **3** selectively to endogenous albumin is almost complete within minutes. Regarding antitumor efficacy and toxicity, it was found that **3** was superior to free doxorubicin in a murine renal cell carcinoma model (RENCA) and in two mamma carcinoma xenograft models in nude mice.[7, 9]

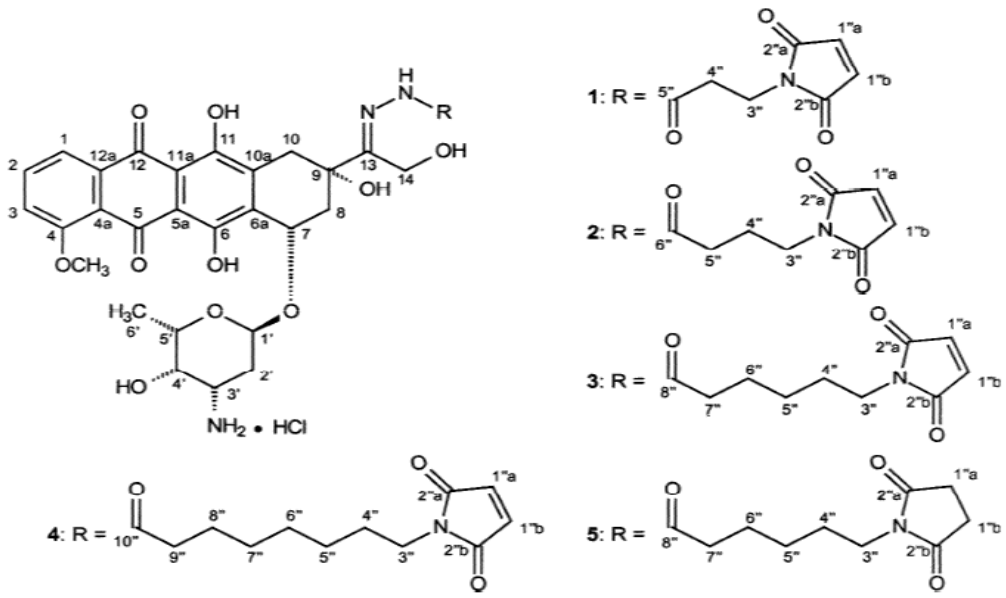

Figure 7. Structures of Doxorubicin Hydrazone Derivatives: **1-5** Containing Aliphatic Maleimide Spacers [7]

Binding of albumin can also be done exogenously. This method also takes advantage of the free thiol group in Cys-34, which can covalently bind to maleimide groups. [10] The first task of this research was design a method for binding albumin to amine terminated nanoparticles (NH_2NP). A heterobifunctional crosslinker with a polyethylene (PEG) spacer for increase flexibility was chosen for linking albumin to the NH_2NP. The crosslinker contained N-hydroxysuccinimide (NHS) ester on one end that reacts with primary amines to form amide bonds, and a maleimide group on the other, which reacts with thiol groups to form stable thioether bonds (Figure 8).[11] The N-hydroxysuccinimide (NHS) ester-PEG_{2000}-Maleimide (NHS-PEG_{2000}-MAL) crosslinker would be bound to NH_2NP. After coupling the linker to the NP, the

double bond of the maleimide group would then be used to bind covalently to the thiol group on Cys-34 of HSA to form a stable thioether bond. The albumin coupling reaction could be conducted *exogenously* or *endogenously*. Albumin binding was monitored via Dynamic Light Scattering (DLS). A measureable increase in particle size was expected as was observed for non-specific binding of ovalbumin to amine-terminated nanoparticles (Figures 9 and 10).

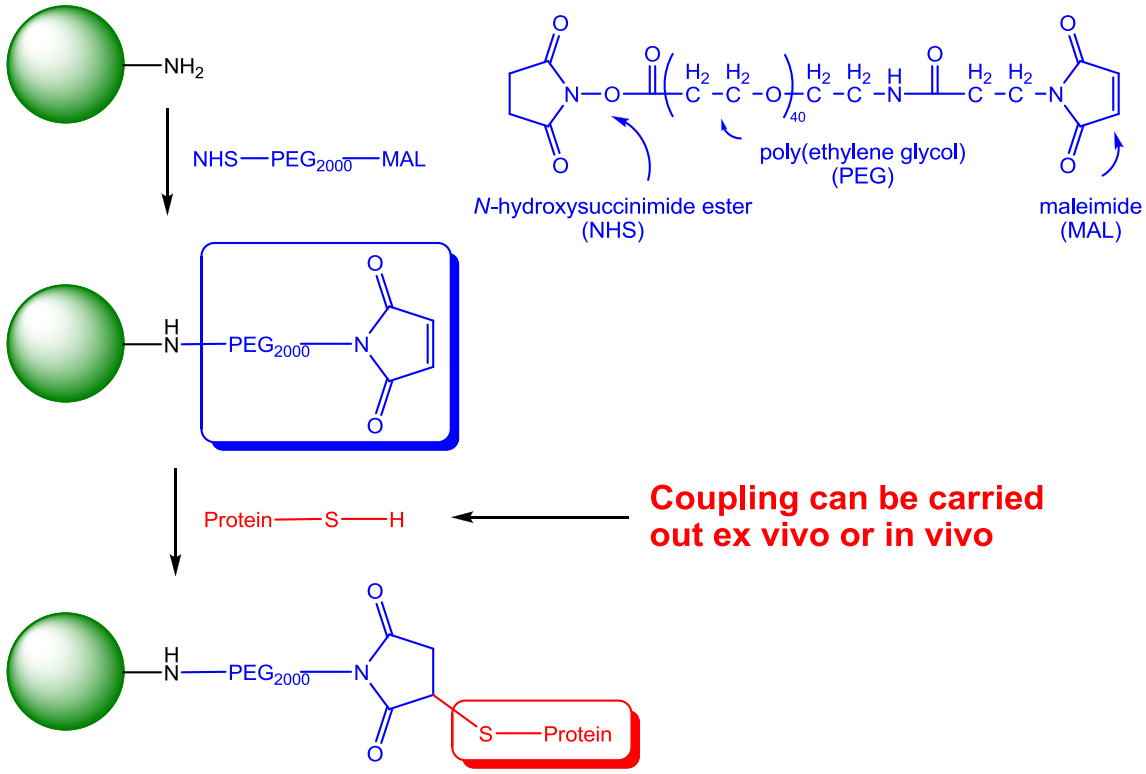

Figure 8. Mechanism for Binding NHS-PEG_{2000}-MAL to NH_2NP

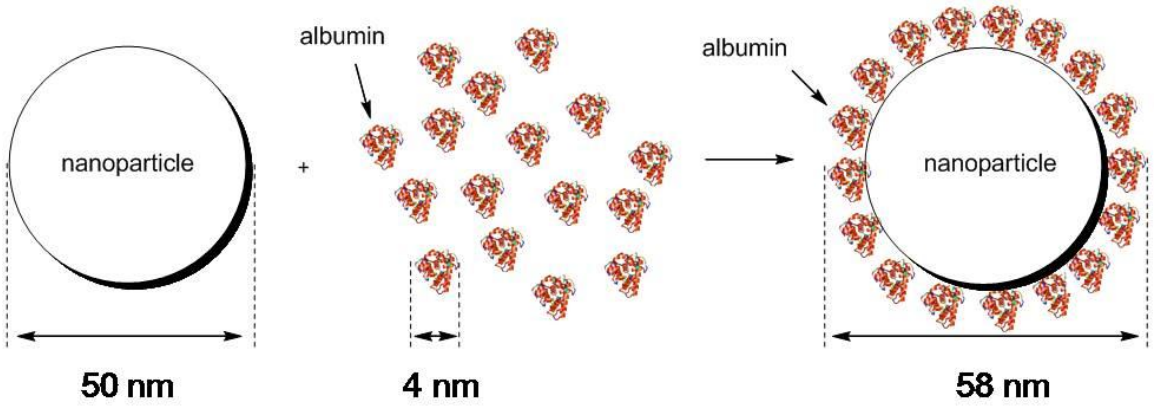

Figure 9. Protein Adsorption on NP Surface: Illustration of the Increase in Particle Size Induced by Protein Adsorption to the Surface of a Nanoparticle
An increase in particle size to 58 nm can be expected if a 50 nm nanoparticle is uniformly coated with albumin, assuming a hydrodynamic radius of approximately 4 nm for albumin.

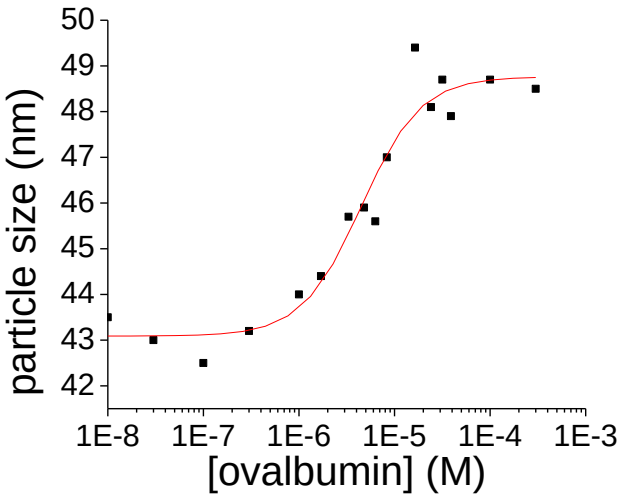

Figure 10. Titration of Amine-Terminated Nanoparticles with Ovalbumin
An increase in particle size of 6.5 nm is observed upon non-specific binding of ovalbumin to the particle surface.

2.2 Experimental

2.2.1 Materials

Albumin from human serum (HSA) purchased from Sigma-Aldrich, Co. According to the manufacturer the purity level of HSA was 96-99% (remainder mostly globulins). Sicastar® NH_2 50 nm 25 mg/mL nanoparticles were ordered from Micromod. Maleimide PEG NHS Ester was purchased from JenKem Technology. 10 000 MWCO Slide-A-Lyzer® Dialysis Cassettes purchased from Thermo Scientific. Spectra/Por® Biotech Cellulose Ester (CE) Dialysis Membrane of 100 000 MWCO was purchased from Spectrum Laboratories, Inc. β–mercaptoethanol was purchased from Sigma-Aldrich, Co.

2.2.2 Binding of Albumin Where Dialysis Was Used as the Purification Method

According to the manufacture's warnings, the NHS-PEG_{2000}-MAL is subject to hydrolytic degradation. Therefore, to avoid decreasing the shelf-life of the crosslinker by moisture from the environment, preparation of the crosslinker solution was carried out in an inert atmosphere glovebox. The model of the glovebox is UNILab© MBraun, and it is equipped with a regenerable purifier unit capable of removing oxygen and moisture from the atmosphere inside the box. The work in the glovebox is performed under an argon atmosphere. The crosslinker solution was prepared by dissolving 3.7 mg of NHS-PEG_{2000}-MAL in 1 mL of deionized (DI) water in an eppendorf tube. The solution was taken out of the glovebox for further use. For a 1000X ratio of crosslinker to NPs, 10 µL aliquot of this solution was taken to react with 50 µL NH_2NPs in 940 µL DI water.

This mixture of crosslinker and NH_2NPs was vortexed for 15 minutes for complete reaction, and then dialyzed in DI water for 1 h to get rid of excess crosslinker and by-products (solvent was changed in half-hour intervals). Before injecting the mixture into the 10 000 MWCO dialysis cassette, the membrane was pre-soaked in water for two minutes as directed in manufacturer's instructions. For the binding of HSA the following methods were explored: Method 1a) 7mg of HSA were dissolved in DI water and 350 µL of this HSA solution was added to the MAL-PEG_{2000}-NHNP solution and vortexed for half-hour. Meanwhile, dialysis tubing 100 000 MWCO was pre-soaked in water for 15 minutes to remove the sodium azide preservative agent, and then thoroughly rinsed with DI water before use. The HSA-MAL-PEG_{2000}-NHNP solution was dialyzed in water overnight, while changing the solvent every 3 h for the first 9 h. Method 1b) Instead of preparing the crosslinker solution in DI water, 2.5% ethanol solution was used as solvent, and the solvent for dialysis was a 15% ethanol solution. However, everything else was followed as in Method 1a.

2.2.3 Albumin Binding Where Centrifugation Was Used for Purification

For these set of experiments a 100X ratio of crosslinker to NPs was prepared by dissolving 3.7 mg of NHS-PEG_{2000}-MAL in 1 mL of DI water, taking 10 µL of this solution and diluting it in 1 mL DI water, and 100 µL aliquot of the diluted solution was reacted with 50 µL NH_2NPs in 850 µL DI water. All other steps of Method 1a were followed, with the exception of overnight dialysis as a means of getting rid of excess unreacted HSA. Instead purification was carried

by the following procedure: 5 cycles of centrifugation using a Centrifuge 5810 R (14 000 rpm, for 8 min at 25 °C), followed by redispersion of pellet using a 2510 Branson Sonicator bath (Temperature set at 40 °C, Sonics 5 min with Heat on). In this section two different methods were also tested: Method 2a) HSA was dissolved in water, while in Method 2b) HSA was dissolved in 50% solution of ethanol.

2.2.4 Albumin Binding with Pre-Quenching of Maleimide Groups

In Method 3a two samples of MAL-PEG_{2000}-NHNP solution were prepared as described earlier in Method 1a (i.e. using 1000X ratio of crosslinker to NPs). The quenching reagent was not added to Sample A, while 10 µL of β–mercaptoethanol was added to Sample B to quench surface maleimide groups. HSA was added to both samples in a series of titrations with the following concentrations: 0.0017 mg/mL, 0.015 mg/mL, 0.14 mg/mL, and 1.2 mg/mL. In Method 3b two samples of MAL-PEG_{2000}-NHNP solution were prepared as described earlier; however instead of using DI water as solvent, a 6% ethanol solution was used. The quenching reagent was not added to Sample C; however, it was added to Sample D as before. HSA was added to both samples as described above.

2.3 Results and Discussion

2.3.1 Dynamic Light Scattering

Particle size characterization was conducted using the Microtrac Nanotrac^{TM} ULTRA, which incorporates the Controlled Reference Method of

analysis of dynamic light scattering for particle sizing. The Nanotrac ULTRA Probe design is optimized to detect particle size distributions in low concentration suspensions and is sensitive to size ranges below 10 nm, however, retains sensitivity to larger sizes up to 6.5 µm and high concentrations. Particle size is determined from the velocity distribution of the particles moving under Brownian motion. In the Nanotrac, light from a laser diode is coupled to the sample through an optical beam splitter in the probe assembly. The interface between the sample and the probe is a sapphire window at the probe's tip. The sapphire window has two functions: First, it reflects the original laser back through the beam splitter to a photodetector. This signal acts as a reference signal for detection. Secondly, the laser passes through the sapphire window and is scattered by the particles which are moving under Brownian motion. The laser's frequency is shifted relative to the velocity of the particle, according to the Doppler Effect. Light is scattered in all directions, and the frequency is transmitted through the sapphire window to the optical splitter in the probe, and to the photodetector. These signals of various frequencies combine with the reflected signal of un-shifted frequency (Controlled Reference) to generate a wide spectrum of heterodyne-difference frequencies. The power spectrum of the interference signal is calculated, and then inverted to give the particle size distribution. [12]

2.3.2 Analysis of Dialysis as Purification Method

2.3.2.1 Analysis of Method 1a

To monitor the reaction taking place, DLS was used for measuring the change in size of the NH_2NPs, which were supplied in a 50 nm size; however, the measured size of the NPs was 45 nm by DLS in the laboratory. The size measured after the NHS-PEG_{2000}-MAL crosslinker was added to the NPs was 42 nm. After dialysis of this solution, the size of MAL-PEG_{2000}-NHNP was 45 nm. This small increase in size, although almost negligible, could be due to completion of reaction between the crosslinker and NH_2NPs. After the addition of HSA, the size measured was 50 nm. The observed increase in size was expected upon protein binding. However, after overnight dialysis of the HSA-MAL-PEG_{2000}-NHNP the data collected from DLS showed that 82% volume of the solution contained 54 nm size NPs, 10% was 1 nm, 5.2% 374 nm and 2.2% 1088 nm. From these results it was speculated that HSA was forming dimers. Figure 11 shows the data collected by DLS.

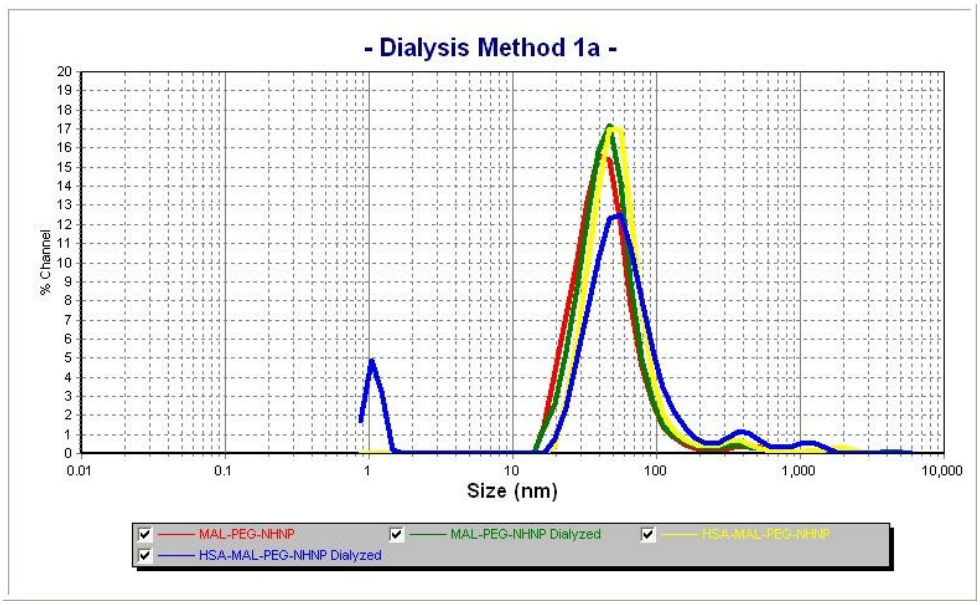

Figure 11. DLS of NPs in DI Water Solvent Dialysis as Purification Method

2.3.2.2 Analysis of Method 1b

As mentioned before, it is known that both the NHS ester and Maleimide groups of the crosslinkers are subject to hydrolysis in aqueous solutions. To reduce the rate of hydrolysis the crosslinker was dissolved in an ethanol solution. The size of the MAL-PEG_{2000}-NHNP before dialysis was 44 nm and after dialysis it was 47 nm. After HSA was added the size measured was 47 nm, which did not reflect the change in size expected. Dialysis was performed using a 15% ethanol solution as solvent. The DLS data collected after overnight dialysis showed that 70% volume of the solution was 613 nm and 30% was 78 nm. Again the increase in size can be accounted by dimerization of HSA. See Figure 12 for summary of DLS data.

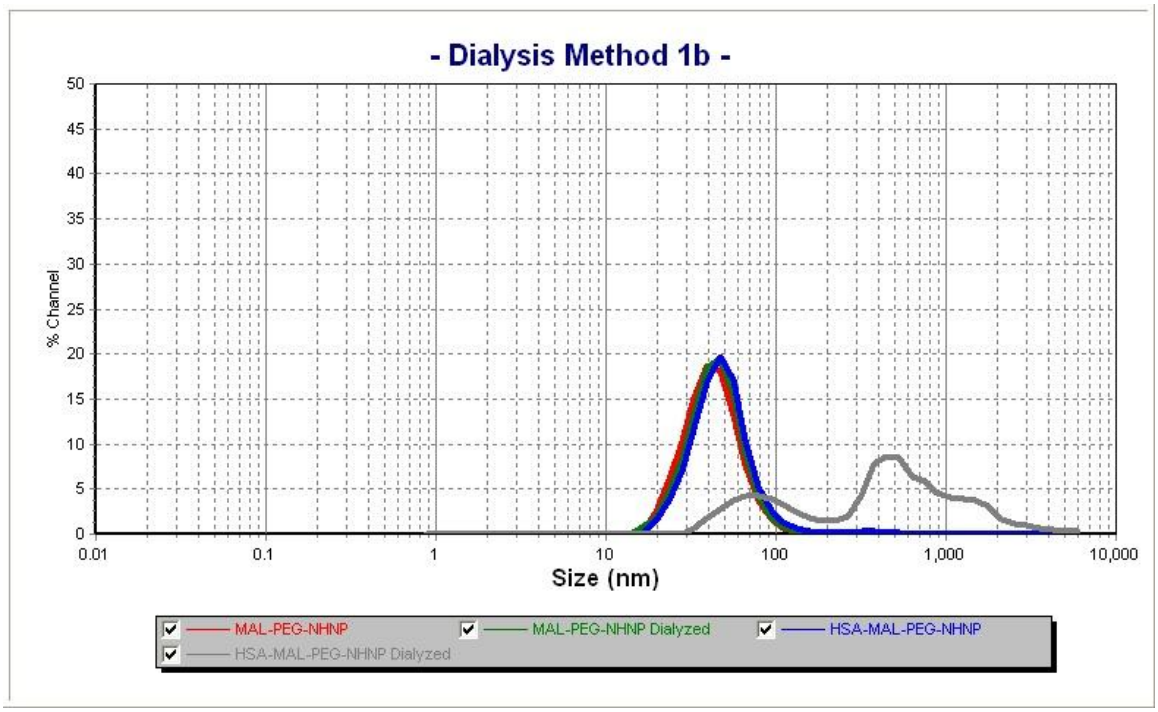

Figure 12. DLS of NPs in Ethanol Solvent Dialysis as Purification Method

2.3.3 Analysis of Centrifugation as the Purification Method

2.3.3.1 Analysis of Method 2a

In Langer and coworker's work, the method used for purification of HSA NPs was done by five cycles of differential centrifugation (20 000 x g, 8 min) followed by an ultrasonication bath for redispersion of the pellet.[13] Based on the previous results, it was decided to try this method. The size of MAL-PEG$_{2000}$-NHNP before dialysis was 41 nm, and after dialysis it was 43 nm. Addition of HSA resulted in 50 nm size. After five cycles of centrifugation analysis of the supernatant by DLS showed 56 nm size NPs, which meant that there were still particles present. The pellet was redispersed by an ultrasonication bath, and NP

size was investigated by DLS. The data showed multiple NP distributions centered at 70 nm, 356 nm, 623 nm, and 1424 nm (see Figure 13 for results).

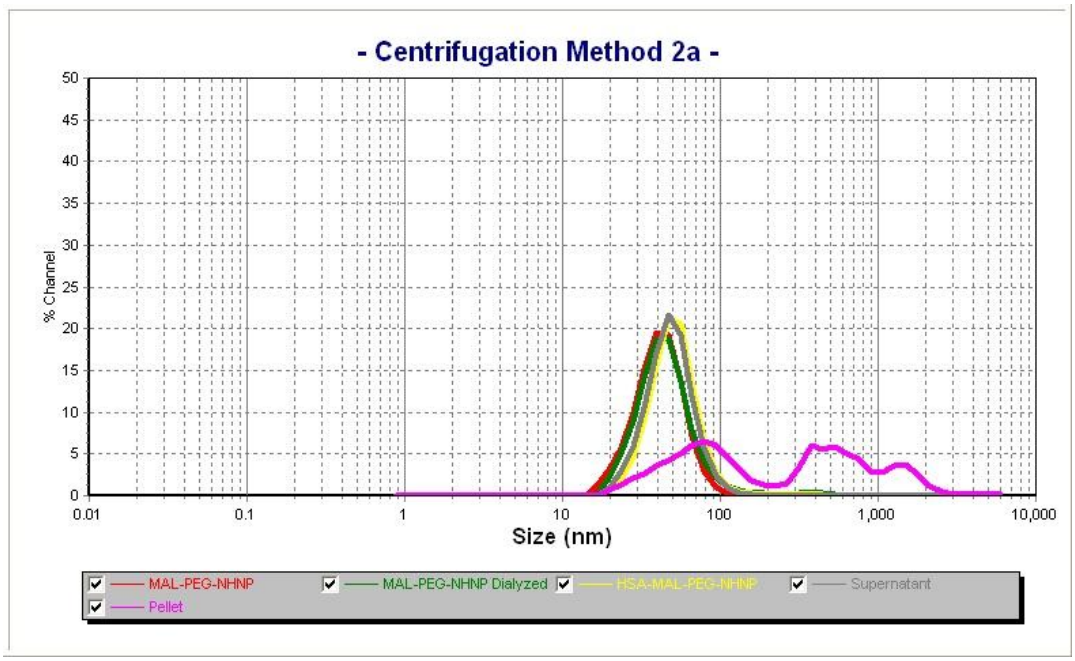

Figure 13. DLS of NPs in DI Water Solvent Centrifugation as Purification Method

2.3.3.2 Analysis of Method 2b

The previous procedure was repeated, but this time HSA was dissolved in an ethanol solution. The size of MAL-PEG_{2000}-NHNP before dialysis was 44 nm, and after dialysis it was 45 nm. These results are consisted with previous results. After addition of HSA, there was a size increase to 67 nm. After centrifugation, analysis of the supernatant resulted in a size of 6 nm which can account for excess monomers or byproducts. Redispersion of pellet was done as in previous experiment, and DLS measured a size of 70 nm. These results point to the possibility of HSA binding to the maleimide group, or that ethanol affects the size of NPs. (see Figure 14 for DLS results)

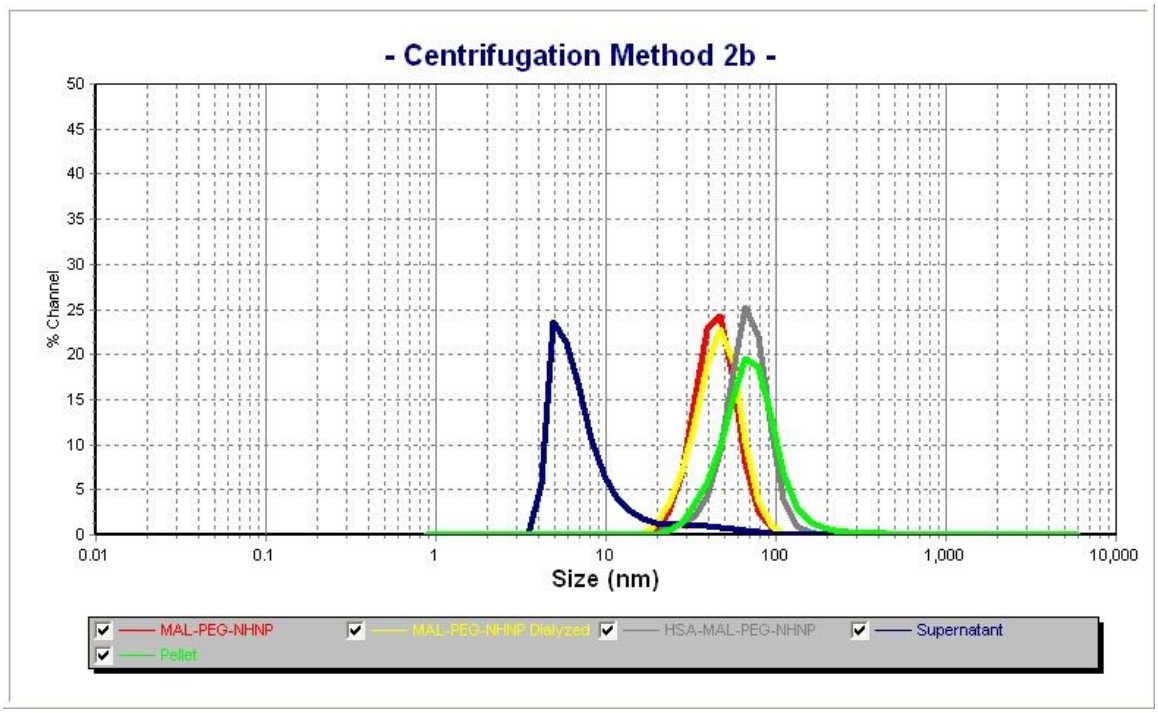

Figure 14. DLS of NPs in Ethanol Solvent Centrifugation as Purification Method

2.3.4 Analysis of Pre-Quenching with Thiol

2.3.4.1 Analysis of Method 3a

To verify that HSA selectively binds to the maleimide group, β-mercaptoethanol was used as a quenching agent. The addition of β-mercaptoethanol would quench the maleimide group, thus preventing the binding of HSA to the particles. For these experiments HSA was added in a series of titrations. Sample A did not contain the quenching agent. The size of MAL-PEG_{2000}-NHNP was 44 nm before dialysis and 45 nm after dialysis. HSA was added as follows and resulted in the following sizes: 0.0017 mg/mL HSA (44 nm), 0.015 mg/mL HSA (45 nm), 0.14 mg/mL HSA (45 nm), 1.2 mg/mL HSA (48 nm). After overnight dialysis size was 450.0 nm (see Figure 15). Sample B

contained 10 µL of β-mercaptoethanol, and the size of the solution was 46 nm after dialysis. HSA was added as follows and resulted in the following sizes: 0.0017 mg/mL HSA (44 nm), 0.015 mg/mL HSA (46 nm), 0.14 mg/mL HSA (45 nm), 1.2 mg/mL HSA (48 nm). After dialysis the measured size was 500.0 nm (see Figure 16). Both Sample A and B produced very similar results, which might mean that not enough quenching agent was added or that HSA is not selective to the maleimide group.

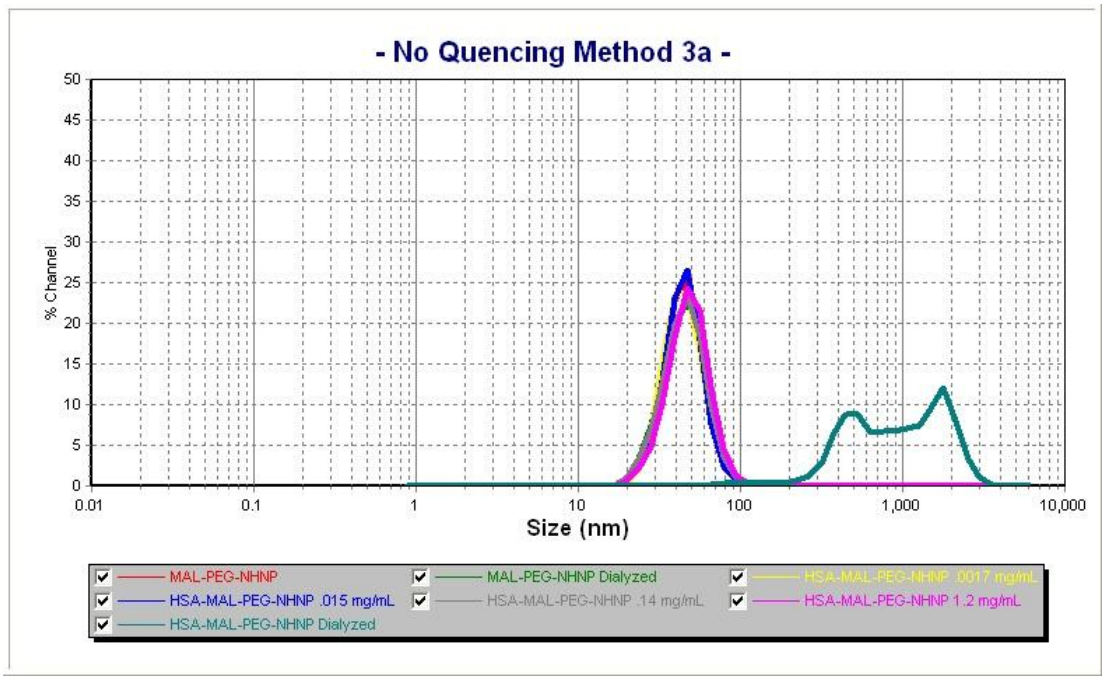

Figure 15. DLS of NPs in DI Water Solvent Without β-Mercaptoethanol

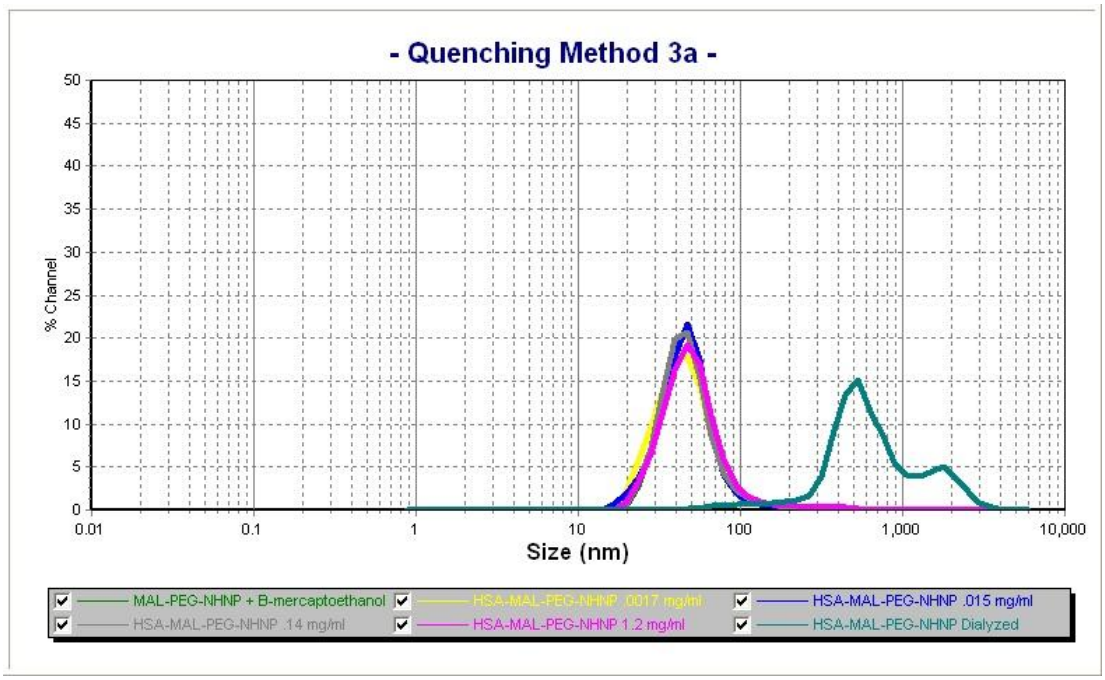

Figure 16. DLS of NPs in DI Water Solvent With β-Mercaptaethanol

2.3.4.2 Analysis of Method 3b

The previous procedure was repeated, but this time the crosslinker was dissolved in an ethanol solution. Sample C did not contain β-mercaptoethanol, and the size before addition of HSA was 44 nm. HSA was added as follows and resulted in the following sizes: 0.0017 mg/mL HSA (44 nm), 0.015 mg/mL HSA (45 nm), 0.14 mg/mL HSA (47 nm), 1.2 mg/mL HSA (49 nm) (Figure 17). Sample D contained 20 µL of β-mercaptoethanol, and the size of the solution was 49 nm after dialysis. HSA was added as follows and resulted in the following sizes: 0.0017 mg/mL HSA (45 nm), 0.015 mg/mL HSA (45 nm), 0.14 mg/mL HSA (47 nm), 1.2 mg/mL HSA (53 nm) (Figure 18). Again both samples produced very similar results, which were inconclusive for showing that HSA is selective for the maleimide group.

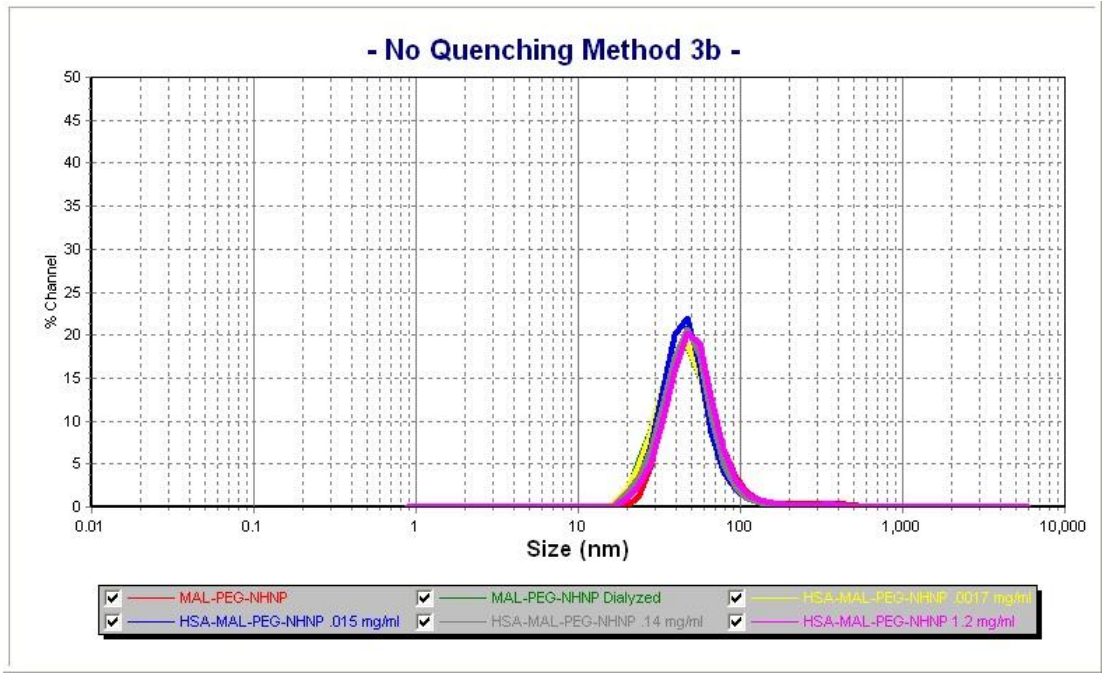

Figure 17. DLS of NPs in Ethanol Solvent Without β-Mercaptoethanol

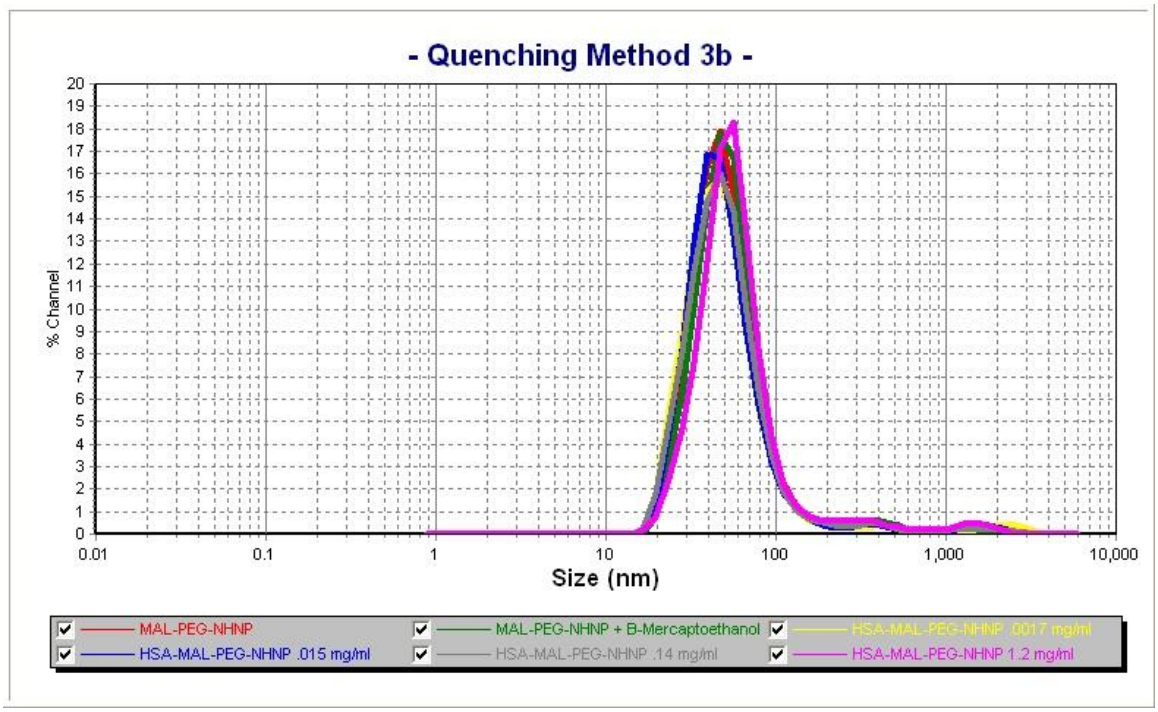

Figure 18. DLS of NPs in Ethanol Solvent With β-Mercaptoethanol

2.4 Conclusions

Unfortunately, DLS results were not conclusive enough to demonstrate that HSA binds to the maleimide functional group. Binding of the crosslinker to the NPs did not seem to pose a problem, because up to that point the results of all experiments were consistent. It was the binding of HSA that was troublesome. In almost all experiments the DLS data pointed towards possible dimerization taking place. Langer and coworkers conducted a study of the batch-to-batch variability of the starting material HSA on the preparation of NPs, and it was found that HSA can form dimers and higher aggregates due to the free thiol group present. Not only does oxidation lead to dimers of HSA, but due to its human origin HSA has other drawbacks such as potential risks of pathogenic contamination and variability in quality. In their study, four batches of HSA (purity 96-99%) were compared for the amount of monomeric and dimeric protein in each batch. According to their results, a correlation between the amount of higher aggregates present in HSA and the resulting particle size and polydispersity seems to exist. [14] These finding could help explain why sizes with 300-1000 nm range were observed. Techniques employed for the purification of the protein-coated NPs were also unsuccessful. In the cases of both purification by dialysis and centrifugation, the NPs tended to agglomerate. Had purification of NPs after reaction of HSA been successful, it may have been possible to distinguish between selective and non-selective protein binding. It was expected that albumin not covalently bound to the NPs would be washed away during

purification. The lack of progress in this project led to the decision of putting it on hold for the moment, and focusing on the synthesis of our own NPs.

2.5 Chapter References

1. Furumoto, K.; Yokoe, J.; Ogawara, K.; Amano, S.; Takaguchi, M.; Higaki, K.; Kai, T.; Kimura, T. *Int. J. Pharm.* **2007,** *329,* 110-116.
2. Liao, L. B.; Zhou, H. Y.; Xiao, X. M. *J. Mol. Struct.* **2005,** *749,* 108-113.
3. Yokoe, J.; Sakuragi, S.; Yamamoto, K.; Teragaki, T.; Ogawara, K.; Higaki, K.; Katayama, N.; Kai, T.; Sato, M.; Kimura, T. *Int. J. Pharm,* **2008,** *353,* 28-34.
4. Ogawara, K.; Furumoto, K.; Nagayama, S.; Minato, K.; Higaki, K.; Kai, T.; Kimura, T. *J. Controlled Release* **2004,** *100,* 451-455.
5. Ogawara, K.; Yoshida, M.; Kubo, J.; Nishikawa, M.; Takakura, Y.; Hashida, M.; Higaki, K.; Kimura, T. *J. Control. Release* **1999,** *61,* 241–250.
6. Karmali, P. P.; Kotamraju, V. R.; Kastantin, M.; Black, M.; Missirlis, D.; Tirrell, M.; Ruoslahti, E. *Nanomedicine: Nanotechnology, Biology and Medicine* **2009,** *5,* 73-82.
7. Kratz, F.; Warnecke, A.; Scheuermann, K.; Stockmar, C.; Schwab, J.; Lazar, P.; Druckes, P.; Esser, N.; Drevs, J.; Rognan, D.; Bissantz, C.; Hinderling, C.; Folkers, G.; Fichtner, I.; Unger,C. *J. Med. Chem.* **2002,** *45,* 5523-5533.
8. Kratz, F.; Muller-Driver, R.; Hofmann I.; Drevs, J.; Unger, C. *J. Med. Chem.* **2000,** *43,* 1253-1256.
9. Kratz, F.; Fichtner, I.; Roth, T.; Fiebig, I; Unger, C. *J. Drug Targeting* **2000,** *8,* 305-318.

10. Santra, M. K.; Banerjee, A.; Rahaman, O.; Panda, D. *Int. J. Biol. Macromol.* **2005,** *37,* 200-204.

11. Thermo Scientific. http://www.piercenet.com/files/1766dh5.pdf (accessed January, 30, 2009), Instructions for SM $(PEG)_n$ Crosslinkers.

12. Microtrac Total Solutions in Particle Size Characterization. http://www.microtrac.com/Home.aspx (accessed May 15, 2010).

13. Langer, K.; Balthasar, S.; Vogel, V.; Dinauer, N.; von Briesen, H.; Schubert, D. *Int. J. of Pharm.* **2003,** *257,* 169-180.

14. Langer, K.; Anhorn, M. G.; Steinhauser, I.; Dreis, S.; Celebi, D.; Schrickel, N.; Faust, S.; Vogel, V. *Int. J. of Pharm.* **2008,** *347,* 109-117.

CHAPTER 3

MICROWAVE IRRADIATION IN FREE RADICAL POLYMERIZATION OF ACRYLATE-BASED POLYMERIC NANOPARTICLES

3.1 Introduction

Nanoparticles (NPs) are particulate systems with diameters ranging from 1 to 1000 nm. As previously mentioned, there is a plethora of different types of NPs being studied for their potential biomedical applications as drug delivery vectors. However, recently researchers have found that synthesizing NPs from polymers provides control over particle size and morphology, as well as spatial stability.[1,2] Therefore, polymeric-NPs have received considerable attention as drug delivery vectors due to their biodegradability, controlled release of drugs, target-specificity, and ability to deliver macromolecules through a per oral route of administration.[3] Thus, an extensive amount of work has been dedicated to developing a convenient method for the synthesis of polymeric-NPs.[3-5]

The two conventional methods of synthesizing polymeric-NPs are dispersion of pre-formed polymers, and polymerization of monomers.[4,5] The dispersion of pre-formed polymers can be further classified into: solvent evaporation, spontaneous emulsification / solvent diffusion, salting out, and the use of supercritical fluid technology.[6] In the solvent evaporation method, the polymer is dissolved in an organic solvent, such as chloroform or ethyl acetate. Then the drug is dispersed into the pre-formed polymer solution, and this mixture

is emulsified with a surfactant into an oil-in-water emulsion. The solvent is evaporated by increasing the temperature/ pressure or by continuous stirring, and this induces polymer precipitation as NPs. The spontaneous emulsification / solvent diffusion method is a modified version of solvent evaporation, in which both water soluble and water insoluble organic solvents are used for spontaneous diffusion. This method leads to smaller NPs. The salting out method was developed to avoid the usage of organic solvents, which are hazardous to the environment and humans. This method is based on the separation of a water-miscible solvent from an aqueous solution via a salting-out effect.[3] The use of supercritical fluids has sparked interest because they are environmentally friendly solvents, and can be used to make high-purity NPs without trace of organic solvents. In this technique the polymer and drug are solubilized in a supercritical solvent, and the solution is expanded through a nozzle. The supercritical fluid is evaporated in the spraying process, and the solute NPs eventually precipitate.[3,6]

On the other hand, polymerization of monomer to form NPs can be further classified into emulsion polymerization and interfacial polymerization.[5,6] Emulsion polymerization is the most common method of synthesizing polymeric NPs.[7,8] There are two types of emulsion polymerization based on the continuous phase employed, either organic or aqueous. The use of an organic continuous phase involves the dispersion of monomer into an emulsion/ inverse microemulsion, or into a non-solvent. Due to the use of toxic organic solvents,

and surfactants, this method has become less popular. In the aqueous continuous phase the monomer is dissolved in an aqueous solution, and there is no need for surfactants or emulsifiers. In either case, polymerization can be initiated by free radicals.[6-8] Finally, interfacial polymerization has the advantage of using polymers that undergo polymerization within seconds. Cyanoacrylate monomers are commonly used for the preparation of drug-loaded NPs via interfacial polymerization. The monomer and drug are dissolved in a mixture of an oil and ethanol, and surfactants if needed. The mixture is then slowly expelled through a needle into a well-stirred aqueous solution. Polymerization of cyanoacrylate is spontaneous after contact with initiating ions present in the water.[6] Since it has been reported that microemulsions enhance the absorption of peptides, the encapsulation of insulin was carried by this method. It was found that nanoencapsulation of insulin by this technique resulted in high entrapment efficiency. The drawback of interfacial polymerization is that to achieve a well dispersed phase suitable for formation of NPs, high input energy in the form of ultrasonication or vigorous stirring is required.[9] Also, even though interfacial polymerization is initiated almost instantaneously, the complete process of synthesizing drug-loaded NPs by this method is still time consuming. For the preparation of NPs, in the insulin study, the reaction system was left for four hours at 4 °C for complete polymerization.[9] Furthermore, in a study of the encapsulation of curcumin, an anti-cancer agent, in polymeric-NPs using an

interfacial free radical polymerization, the polymerization was performed at 30 °C for 24 hours.[10]

Some of the hurdles of surfactant-free emulsion polymerization (SFEP) include: the preparation of monodisperse, sub-100 nm NPs at high solids content, and the incorporation functional groups and cross-links in NPs. To overcome these challenges a facile microwave methodology was reported by An and co-workers. The authors found that, in contrast to thermal heating, microwave irradiation offers unique size control and reduces the reaction time to as short as 30 min. Varying the temperature or microwave power resulted in a range of diameter size (100-300 nm). Although microwave irradiation does not initiate polymerization, it was implied that the microwave irradiation can dielectrically couple with the initiator anions to accelerate decomposition to radicals thus enhancing radical influx in the solution. This method of microwave synthesis proved to be a powerful tool for the production of cross-linked, functionalized NPs under high solids content and surfactant-free conditions.[11]

In an effort to synthesize functionalized NPs that are suitable for drug delivery, this work explored microwave irradiation for the free radical polymerization (FRP) of acrylate monomers similar to those in the literature (see Figure 19 for FRP Mechanism) .[11] Like other chain growth mechanisms, FRP involves the sequential addition of vinyl monomers to an active, free radical center. The basic FRP mechanism includes initiation, propagation and termination; details of the mechanism can be found throughout the literature.[12]

Briefly, the free radicals that initiate polymerization are generated by thermal or photochemical homolytic cleavage of covalent bonds of initiators. Common initiators include azo and peroxy compounds. The initiator decomposes to form two radicals; and chain initiation occurs when the radical adds to the monomer. Chain propagation continues via successive addition of monomer units to the radical center. Bimolecular coupling of two growing chains results in loss of two radicals, which leads to termination. Chain termination can occur by either combination, formation of one dead polymer chain, or by disproportionation, formation of two dead polymer chains.[12]

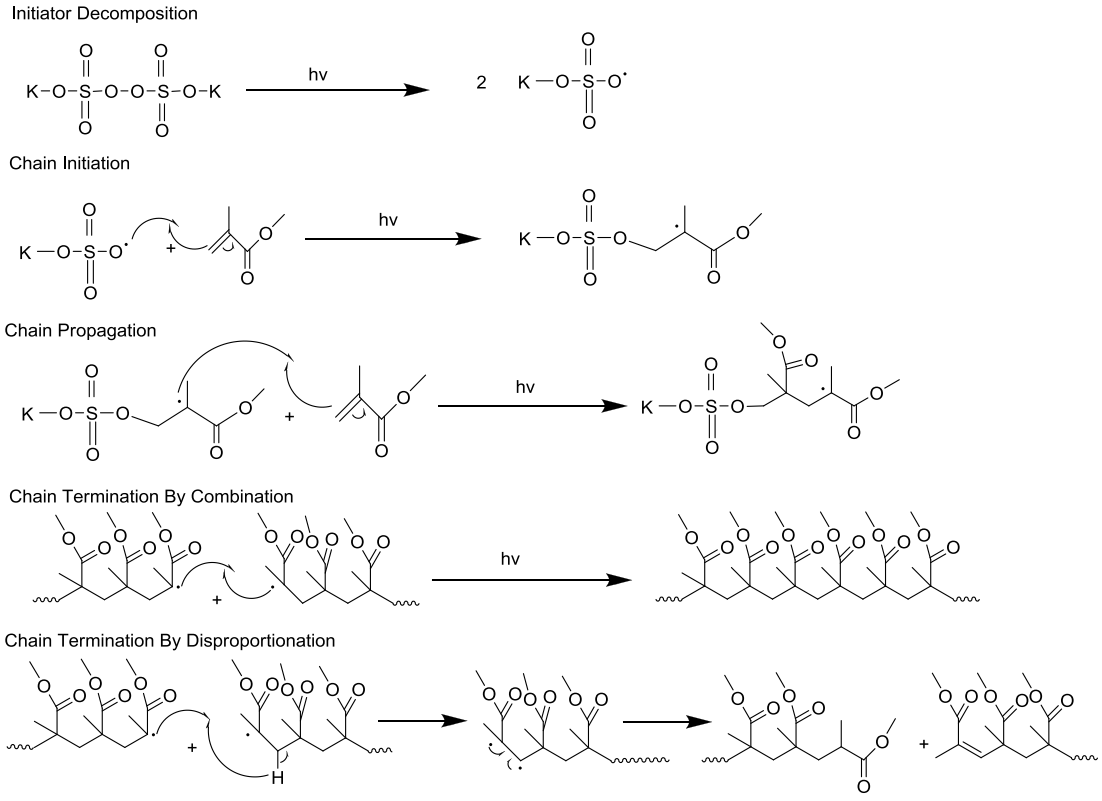

Figure 19. Free Radical Polymerization Mechanism of MMA

The polymerization of methyl methacrylate (MMA) was initiated by the initiator potassium persulfate (KPS). Acrylic acid was added to provide a functional group on the surface of the NPs for conjugation reactions, and the crosslinker PEG_{200}-diacrylate (PEG-DA) was used to enhance NP stability. The chemical structures of PEG-DA, AA, MMA, and a partial structure of the acrylate-based NP are shown in Figure 20. Several experiments were carried to analyze the following reaction parameters and their effect on NP size: temperature, microwave power, reaction time, initiator concentration, and percentage of monomer used. The software SAS Design of Experiment (Box-Behnken model) was used to design a set of experiments that varied the aforementioned parameters. The goal of the first set of experiments was to find the ideal parameters for the synthesis 50 nm NPs, and verify reproducibility of synthesis using commercially available 50 nm NPs as the standard. Our attention then shifted to high throughput approach for the synthesis of 120 nm NPs that would be the base particle of our drug delivery vector. High throughput synthesis of NPs was done on both small and large scales. Lyophilization of NP-containing solutions was employed as a means of removing the particles from solution, which allowed their mass to be determined while still facilitating their re-dispersal into solution without NP agglomeration. This also allows NPs to be stored in a dry state, thus increasing their shelf-life. Finally, NPs labeled with a fluorophore were synthesized for future in vitro and in vivo assays of the NPs, where fluorescence is used to probe NP activity.

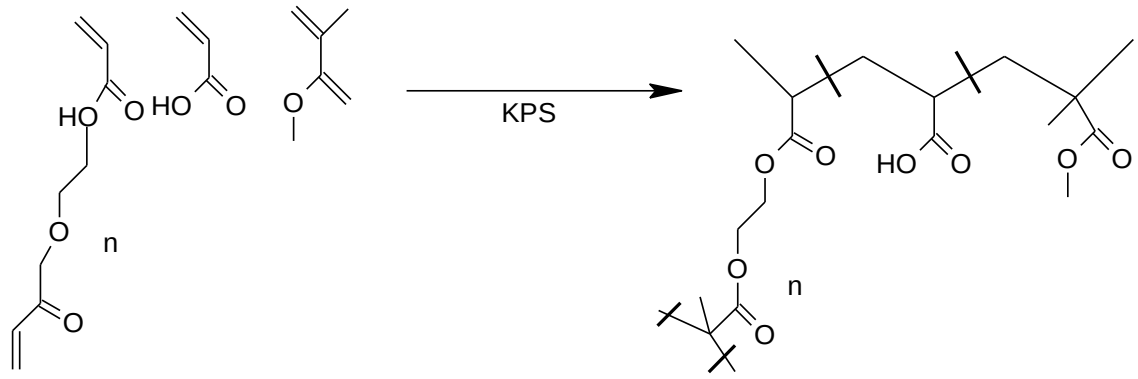

Figure 20. Chemical Structures of Monomers and Partial Structure of NP

3.2 Experimental

3.2.1 Materials

Potassium persulfate (FW 270.33, d 2.477) ordered from Aldrich Chemical Company, Inc. Methyl Methacrylate (MW 100.1 Sp. g. 0.94), Acrylic Acid (MW 72.1 Sp. g. 1.045), Poly(Ethylene glycol)(200) Diacrylate (Sp. g. 1.12) all from ordered from Polysciences, Inc. Fluorescein o-acrylate (FW 386) was purchased from Sigma-Aldrich, Co. Seamless-Cellulose Dialysis Tubing (12 000 MW cut-off) was purchased from Fisher Science Education. NALGENE Syringe Filters with Nylon Membranes 0.2 Mic., 25mm, Fisherbrand 25 mm Syringe Filters 0.2 µm were from Fisher Scientific, and Aluminum oxide (MW 101.96) was from Sigma- Aldrich, Co.

3.2.2 Synthesis of Nanoparticles with CEM Microwave

Microwave irradiation enhances free radical polymerization of monomer dissolved in aqueous solution. Methyl Methacrylate (MMA), acrylic acid (AA) and the cross-linker PEG_{200}-diacrylate (PEG-DA) were each ran through an aluminum

oxide column for purification. NPs were synthesized from MMA, AA, and PEG-DA in solutions containing 4mL of deoxygenated ultrapure water (water was pre-purged with nitrogen for at least 30 min) containing the heat activated initiator potassium persulfate (KPS). The synthesis was carried out in a CEM LabMate Microwave which features the IntelliVent^{TM} Pressure Control System. IntelliVent offers an automated overpressure venting capability. The microwave is also equipped with Window®-based Syngery software that is user friendly and allows for parameter control. The maximum power at which the microwave operates is 200 W. The microwave was set to closed vessel mode, and temperature was measured via an infrared temperature sensor. The following parameters were varied to investigate their effect on NP size: temperature, microwave power, reaction time, initiator concentration, and % solids, which is the total amount of monomers in solution.

3.2.3 Synthesis of Nanoparticles on Small Scale

High throughput synthesis of NPs allows for the preparation of larger quantities of particles in short amounts of time. This approach was made possible by the Microwave Synthos 3000 which offers temperature homogeneity, a self-acting cooling system, simultaneous pressure sensing for 8 vessels, wireless sensors for reaction control, and a maximum power of 1400 W. Also, different rotors can be employed such as the Rotor 64MG5, which fits 64 vials each capable of holding 5 mL of solution. This particular rotor was used for testing a large number of different samples simultaneously. The water used for

these samples was degassed through series of freeze, pump, and thaw cycles. The deoxygenated water and all other reagents were taken inside an inert atmosphere glovebox, and the preparation of the samples was carried out inside the glovebox to avoid exposure to adventitious oxygen. The NPs were synthesized from mixtures of MMA, AA, and PEG-DA in 3 mL of deoxygenated water containing KPS initiator. The microwave settings were Power 300 W, IR temperature of 67° C (80 °C according to the manufacturer's temperature conversion), fan 1, and reaction time was 30 minutes.

3.2.4 Synthesis of Nanoparticles on Large Scale

Like in the preceding section, all preparation for NPs was done inside the glovebox. However, the volume of the samples was increased to 30 mL. Synthesis was done with the same microwave, but a Rotor 16MF100 was used instead of the Rotor 64MG5. Although Rotor 16MF100 can only hold 16 vessels, each vessel can hold up to 100 mL of solution. Since the volume was increased by a 10-fold, it took longer for the microwave to reach the reaction temperature of 55°C IR. Therefore, the microwave was first set at 1400 W, IR = 90° C, fan at 1 to ramp up the temperature to IR = 53° C, and then the settings were changed to 1400 W, fan at 1, IR = 55° C to maintain constant temperature of IR = 55° C for 20 minutes. After 20 min, the power was changed to 0 W and fan at 3 for 10 min for cooling.

3.2.5 Synthesis of Fluorescently Labeled Nanoparticles

Preparation of the fluorescently-labeled NPs was conducted as described in the previous section with slight modifications. Three milligrams of fluorescein-o-acrylate was added to each sample, and the volume in each vessel was increased to 60 mL. For the addition of the fluorescent label, 12 mg of fluorescein-o-acrylate was dissolved in 50 µL of dimethyl sulfoxide (DMSO), and 12.5 µL of this solution was added to each sample.

3.3 Results and Discussion

3.3.1 Analysis of Nanoparticles Synthesized with CEM Microwave

3.3.1.1 Experiments Designed by SAS Design of Experiments Software

A set of 46 experiments were designed using the SAS Design of Experiment (Box-Behnken model) software (Table 1). These samples were run one at a time for either 2 or 3 minutes microwave time. The purpose of these experiments was to investigate how NP size was affected by power, initiator concentration, % AA, % PEG-DA, and % solids. In order to generate the set of experiments, a centerpoint, which has every factor at its central value, must be determined. The centerpoint for these reactions was power of 10 W, 0.18 M KPS, 13% AA, 5% PEG-DA, and 1.25% solids. This centerpoint was chosen because under these conditions, the NPs synthesized were approximately the target size of 50 nm. Unfortunately, no obvious trend was observed regarding the effect on NP size as each parameter was changed. There was a slight increase in size as power was increased, but it was almost negligible. Table 1

contains the parameters for each run as well as the resulting size of the NPs produced under those conditions.

Table 1. Size in nm of NPs Synthesized Using Design of Experiments

Factor	**Low**	**Center**	**High**
POWER	8	10	12
KPS (M)	0.15	0.18	0.21
%AA	9.75	13	16.3
%PEG-DA	3.75	5	6.25
% SOLIDS	0.938	1.25	1.56

POWER	KPS	AA	PEG-DA	SOLIDS	TIME	SIZE
8	0.15	13	5	1.25	3	75
8	0.18	9.75	5	1.25	3	72
8	0.18	13	3.75	1.25	3	83
8	0.18	13	5	0.938	3	75
8	0.18	13	5	1.56	3	85
8	0.18	13	6.25	1.2	3	81
8	0.18	16.3	5	1.25	3	65
8	0.21	13	5	1.25	3	75
10	0.15	9.75	5	1.25	2	65
10	0.15	13	3.75	1.25	2	74
10	0.15	13	5	0.938	2	46
10	0.15	13	5	1.56	2	57
10	0.15	13	6.25	1.25	2	52
10	0.15	16.3	5	1.25	2	64
10	0.18	9.75	3.75	1.25	2	38
10	0.18	9.75	5	0.938	2	60
10	0.18	9.75	5	1.56	2	52
10	0.18	9.75	6.25	1.25	2	42
10	0.18	13	3.75	0.938	2	59
10	0.18	13	3.75	1.56	2	68
10	0.18	13	5	1.25	2	55
10	0.18	13	5	1.25	2	63
10	0.18	13	5	1.25	2	51
10	0.18	13	5	1.25	2	61
10	0.18	13	5	1.25	2	56
10	0.18	13	6.25	0.938	2	59
10	0.18	13	6.26	1.56	2	62

10	0.18	16.3	3.75	1.25	2	72
10	0.18	16.3	5	0.938	2	91
10	0.18	16.3	5	1.56	2	55
10	0.18	16.3	6.25	1.25	2	67
10	0.21	9.75	5	1.25	2	69
10	0.21	13	3.75	1.25	2	65
10	0.21	13	5	0.938	2	57
10	0.21	13	5	1.56	2	65
10	0.21	13	6.25	1.25	2	69
10	0.21	16.3	5	1.25	2	68
12	0.15	13	5	1.25	2	79
12	0.18	9.75	5	1.25	2	87
12	0.18	13	3.75	1.25	2	88
12	0.18	13	5	0.938	2	82
12	0.18	13	5	1.56	2	91
12	0.18	13	6.25	1.25	2	84
12	0.18	16.3	5	1.25	2	93
12	0.21	13	5	1.25	2	80

3.3.1.2 Software-Predicted Parameters for the Synthesis of NP of a Given Size

Based on the NPs size measured, the SAS DOE software has a feature that can calculate the necessary parameters to maximize, minimize, or optimize the synthesis of NPs of a desired size. We used the software to predict the parameters for synthesizing the largest NPs possible, the smallest NPs possible, and NPs that were 50 nm in diameter (Table 2). The parameters estimated for the maximum NP size were off by 37 nm, when compared to the actual value measured. The actual value for the minimum size was significantly smaller than the projected size; however, the optimization parameters for 50 nm NPs gave a result that was close to the projected value. These experiments were conducted several times and the results in Table 2 represent the best fit between predicted and experimental values.

Table 2. Actual Size in nm of Maximized, Minimized, and Optimized NPs

Power	Time	KPS	% AA	% PEG-DA	% Solids	Size	Actual Size
12	2	0.15	16.3	3.75	1.09	112.37[a]	76
10	2	0.15	9.75	6.25	0.938	46.25[b]	38
10	2	0.15	9.75	6.25	1.25	50.09[c]	49

[a] Maximized NP, [b] Minimized NP, [c] Optimized NP

3.3.1.3 Percent Conversion of Monomer

Percent conversion of monomer to polymer is an important feature of the polymerization that warranted investigation. To this end a sample was prepared under the following parameters of 0.18 M KPS, 16.25% AA, 5% PEG-DA, 78.75% MMA, 1.25% solids, constant temperature of 80 °C, for 30 minutes. The size of the NPs was 136 nm. The solution of particles was then centrifuged for 4 h (14 000 rpm, 4°C), and the pellet was redispersed and washed with acetone. After three washings the particles were centrifuged again for 4 h. The pellet was then left to dry overnight using a vacuum. The percent conversion was calculated 86%, and the second time the procedure was repeated it was 97%. This was a substantial improvement over initial experiments at short reaction times, where percent conversion was as low as 19% when the reaction was run for only 2 minutes. To increase the percent conversion we gradually increased the reaction time from 2 min to 10, 15, and finally 30 min, and the calculated percent conversions improved to 61%, 66%, and 86%, respectively.

3.3.1.4 Factors Affecting NP Size

The effects of % solids, % PEG-DA and KPS concentration on NP size were studied by using the preceding parameters as a control (136 nm NP size). Doubling the % solids did not change the NP size significantly (see Table 3). Increasing %PEG-DA to 30%, however, resulted in a decrease in NP size, (see Table 4). The doubling of KPS concentration also lead to small decrease in size (see Table 5). An and coworkers also reported a decrease in particle size as they increase KPS concentration, however they saw an increase in size as crosslinker was increased.[11]

Table 3. Size in nm of NPs when Doubling % Solids

	Avg. NP Size (nm)[a]
1.25% solids	136
2.5% solids[b]	134

[a] Parameters kept constant: Temperature 80 °C, KPS 0.18 M, 16.25% AA, 5% PEG-DA, 78.75% MMA, and 30 min reaction time.
[b] The NP sizes in nm of 4 individual runs were: 123, 128, 136, and 151.

Table 4. Size in nm of NPs when % PEG-DA Increases

	Avg. NP Size (nm)[a]
5% PEG-DA	136
30% PEG-DA[b]	100

[a] Parameters kept constant: Temperature 80 °C, KPS 0.18 M, 16.25% AA, 78.75% MMA, 1.25% solids and 30 min reaction time.
[b] The NP sizes in nm of 8 individual runs were: 105, 108, 114, 122, 112, 112, 113 and 117.

Table 5. Size in nm of NPs when Doubling KPS

	Avg. NP Size (nm)[a]
0.18 M KPS	136
0.36 M KPS[b]	124

[a] Parameters kept constant: Temperature 80 °C, KPS 0.18 M, 16.25% AA, 5% PEG-DA, 78.75% MMA, 1.25% solids and 30 min reaction time.
[b] The NP sizes in nm of 4 individual runs were: 115, 119, 127 and 135.

3.3.2 High Throughput Analysis of Small Scale Production of Nanoparticles

3.3.2.1 Experiments Designed by SAS Design of Experiments Software

High throughput synthesis was first conducted by using a 64MG5 Rotor, which can hold 64 vials with 3 mL of solution in each, and can therefore produce 192 mL of NP-containing solutions. The SAS DOE (Box Behnken model) was used to design a set of 27 experiments with the centerpoint of 2.3% solid, 50% AA, 5% PEG-DA, 45% MMA and 0.18 M KPS (see Table 6). For the first trial two samples of each of the 27 experiments and 10 samples of the centerpoint were prepared for a total load of 64 vials, however, every sample formed precipitates with samples forming NPs. It was speculated that this result was due to the long time it took to prepare all 64 samples. Therefore, for the next run only 16 samples were prepared and only one of those formed precipitates. The next run was 32 samples, and with the exception of three, all samples formed precipitates. We then decided to limit the number of samples run concurrently to 16 and test whether the results were reproducible. Unfortunately, the particle sizes measured in the second run did not match those of the first run.

Table 6. Sizes in nm of NPs Synthesized Using Design of Experiment

% SOLIDS	% AA	% PEGDA	KPS (M)	Trial 1-Size (nm)	Trial 2-Size (nm)	Trial 3-Size (nm)
1.84	40	5	0.18	134	pcpts	113
1.84	50	4	0.18	144	pcpts	144
1.84	50	5	0.144	117	pcpts	131
1.84	50	5	0.216	155	pcpts	195
1.84	50	6	0.18	160	pcpts	178
1.84	60	5	0.18	207	pcpts	pcpts
2.3	40	4	0.18	163	pcpts	182
2.3	40	5	0.144	148	pcpts	168
2.3	40	5	0.216	115	pcpts	218
2.3	40	6	0.18	215	190	187
2.3	50	4	0.144	157	192	165
2.3	50	4	0.216	pcpts	pcpts	239
2.3	50	5	0.18	145	pcpts	204
2.3	50	5	0.18	164	pcpts	275
2.3	50	5	0.18	183	pcpts	274
2.3	50	6	0.144	226	pcpts	185
2.3	50	6	0.216		pcpts	
2.3	60	4	0.18		pcpts	
2.3	60	5	0.144		pcpts	
2.3	60	5	0.216		pcpts	
2.3	60	6	0.18		pcpts	
2.76	40	5	0.18		260	
2.76	50	5	0.144		pcpts	
2.76	50	5	0.216		pcpts	
2.76	50	4	0.18		pcpts	
2.76	50	6	0.18		pcpts	
2.76	60	5	0.18		pcpts	
2.3	50	5	0.18		pcpts	
2.3	50	5	0.18		pcpts	
2.3	50	5	0.18		pcpts	
2.3	50	5	0.18		pcpts	
2.3	50	5	0.18		pcpts	

3.3.2.2 Optimizing Functional Group Content and Percent Solids

The NPs synthesized have a carboxylate functional group throughout the particle that will be used to conduct subsequent conjugation reactions. To increase the amount of functional groups, the percentage of AA was increased. We were also interested in maximizing the amount of nanoparticles synthesized in terms of weight percent of solution (%solids). Therefore, the effect of % solids and % AA on NP size was studied (see Table 7). In general, as % solids increased the particle size increased as well, although there was a slight decrease going from 3 to 5 % solids. Conversely, as % AA increased there appeared to be a decrease in particle size in most instances, which is consistent with the findings of An and coworkers, who found that an increase in comonomer lead to a decrease in NP size. Their study used 2-hydroxyethyl methacrylate (HEMA) as comonomer with MMA, and as % HEMA increased from 0% to 15% the NP size decreased from ~70 nm to ~30 nm.[11]

Table 7. Size in nm of NPs as %Solids and %AA Increase

% Solids[a]	%AA	Size (nm)	%AA	Size (nm)	%AA	Size (nm)
1.25	50	81	75	49	95	1.0
2.13	50	125	75	1.0	95	1.0
3	50	156	75	226	95	4.0
5	50	93	75	pcpts	95	3.0

10	50	pcpts	75	pcpts	95	pcpts

[a] PEG-DA percentage was kept constant at 5% for all samples

3.3.2.3 Effect of Stir Time on NP Size

In most conventional methods of synthesizing polymeric NPs, vigorous stirring is employed; therefore experiments were conducted to test the effect of stir time on NP size. The following parameters were kept constant: 2.23% solids, 50% AA, 5% PEG-DA, 45% MMA, 0.18 M KPS; and only the stirring times were changed. Table 8 summarizes results. If the reaction was stirred for more than 3 minutes precipitates were formed. Varying the time from 1 minute to no stirring at all, however, did not produce a general trend in NP size.

Table 8. Size in nm of NPs Varying Stirring Times

Stir time (s)	Average NP size (nm)
0	174
15	180
30	194
60	109
180	126
300	pcpts

3.3.3 Analysis of Large Scale Production of Nanoparticles

3.3.3.1 Effect of Percent Solids on NP Size

In the first set of experiments, the increase of % solids and its effect on NP size was studied. The following parameters were kept constant: IR temp = 55 °C, 50% AA, 5% PEG-DA, 45% MMA and 0.1 M KPS. Percentage of solids was increased from 1 to 4% (see Table 9). It was observed that as % solids increased the NP size increased as well. Conversion of monomer was calculated by lyophilizing a 3 mL sample of the 4% solids NP solution (164 nm). Lyophilization is carried out using the principle of sublimation, in which a substance goes from the solid phase directly to the vapor phase. For the lyophilizing procedure, a 3 mL sample was dialyzed for 4 h. The sample was then frozen in liquid nitrogen, and lyophilized with a FreeZone 2.5 Liter Lyophilizer for 24 h. Conversion of monomer was calculated to be 77% using this method. To check for the stability of the NPs to lyophilization, as well as their propensity to re-disperse, which is an issue when purification is accomplished via centrifugation, a 1.8 mg sample was re-dispersed in 3 mL DI water and the size was measured. Two samples were prepared with measured sizes of 161 nm for the first sample, and 166 nm for the second sample. These values match closely to that of the original size, 164 nm. Thus dialysis/lyophilization can be used to purify and increase the shelf-life of NPs without limiting their re-dispersion.

Table 9. Size in nm of NPs Varying % Solids

% Solid	% AA	%PEG-DA	Size
1	50	5	95
1	50	5	98
2	50	5	141
2	50	5	146
3	50	5	138
3	50	5	166
4	50	5	159
4	50	5	164

3.3.3.2 Effect of Percent AA on NP Size

Next, we again looked at the effect of increasing % AA and its effect on NP size. The following parameters were kept constant: IR temp = 55 °C, 2% solids, 5% PEG-DA, and 0.1 M KPS. Percentage of AA was increased from 20 to 80% (see Table 10 for results). Size did not seem to be affected by increase of %AA. This is not consistent with our results above, or with the findings of An and coworkers who found that an increase in comonomer (MMA + HEMA) leads to a decrease in NP size.[11]

Table 10. Size in nm of NPs % AA Increase

% Solid	% AA	%PEG-DA	Size (nm)
2	20	5	135
2	40	5	140
2	60	5	145
2	80	5	pcpts

3.3.4 Analysis of Fluorescently-labeled Nanoparticles

The synthesis of NPs containing a fluorophore was accomplished by adding a fluorescent monomer, fluorescein-o-acrylate, to the monomer mixture.

The parameters were 1% solids, 60% AA, 5% PEG-DA, 35% MMA 0 .1 M KPS, 3 mg fluorescein-o-acrylate, in a total volume of 60 mL. Compared to the 1% solid NPs synthesized before (95 nm and 98 nm, Table 9) the increase in volume and addition of fluorescent label did not have much of an impact on size. Table 11 shows the size of four samples of fluorescently-labeled NPs synthesized. By simple observation it was obvious that the fluorescein label had been incorporated, because the solutions were a yellow color, instead of the usual colorless appearance. The particles were purified and lyophilized, as described above, and the percent conversion was calculated. The theoretical maximum was 2.4 g of NPs, however, the purified NP weight was 1.5506 g after lyophilization, which yields 65% conversion. To check for fluorescence, both fluorescently-labeled and un-labeled NPs were examined by fluorescence microscopy. (see Figure 21a-d)

Table 11. Size in nm of Fluorescently-labeled NPs

% Solid	% AA	%PEG-DA	Size (nm)
1	60	5	92
1	60	5	92
1	60	5	96
1	60	5	96

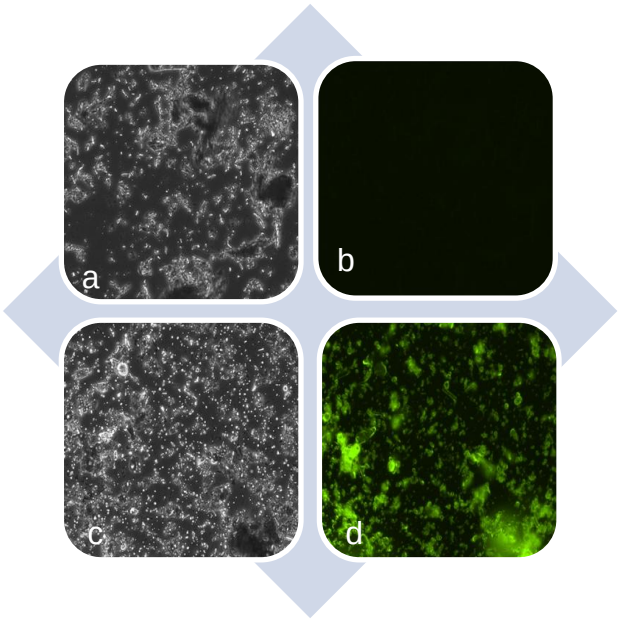

Figure 21a-d Comparisons of Fluorescently Labeled NPs and Un-labeled NPs

[a] NP w/o Fluorescein DIC [b] NP w/o Fluorecein Fluorescence
[c] NP w/ Fluorescein DIC [d] NP w/ Fluorecein Fluorescence

3.4 Conclusions

Although the high level of control over NP size that was cited in the paper by An et al. was not observed in these studies, microwave assisted synthesis of NPs greatly reduces the reaction time and allows for large quantities of NPs to be conveniently synthesized. The longest reaction time employed here was for 30 minutes. In contrast, a conventional thermal heating method for the polymerization reaction was reported to last 12 h.[11] Reasonable percent conversion of monomer to NP was achieved ranging from 65-97%. Reactions conducted in the CEM LabMate Microwave were fairly reproducible; however, only one sample of 4 mL could be run at a time limiting large-scale synthesis and

high throughput testing. On the other hand, the Synthos 3000 allowed larger volumes of NPs to be synthesized in the same amount of time. Use of the Rotor 64MG5 did not provide the anticipated advantages in high throughput chemistry, probably because of the long time it took to prepare all 64 samples. The best results were obtained when a maximum of 8 samples were run simultaneously. With the Rotor 16MF100, however, larger volumes of NP were produced and the results were more consistent. The synthesis of fluorescently-labeled NPs was accomplished successfully, and purification by a combination of dialysis and lyophilization was found to be an effective method for increasing the shelf-life of NPs without affecting their stability. In this study, ~1.5 g of fluorescently-labeled, carboxylic acid-functionalized NPs were synthesized (100 nm diameter) for a total cost of less than $1. The same quantity of NPs of similar size and composition would cost over $4,000 if purchased from Micromod, a commercial supplier of NPs for research.

3.5 Chapter References

1. Rozenberg, B. A.; Tenne, R. *Progress in Polymer Science* **2008,** *33,* 40-112.

2. Liu, S.; Wei, X.; Chu, M.; Peng, J.; Xu, Y. *Colloids and Surfaces B: Biointerfaces* **2006,** *51,* 101-106.

3. Soppimath, K. S.; Aminabhavi, T. M.; Kulkarni, A. R.; Rudzinski, W. E. *J. Controlled Release* **2001,** *70,* 1-20.

4. Hans, M. L.; Lowman, A. M. *Current Opinion in Solid State and Materials Science* **2002,** *6,* 319-327.

5. Akagi, T.; Baba, M.; Akashi, M. *Polymer* **2007,** *48,* 6729-6747.

6. Pinto Reis, C.; Neufeld, R. J.; Ribeiro, António J.; Veiga, F. *Nanomedicine: Nanotechnology, Biology and Medicine* **2006,** *2,* 8-21.

7. Feng, H.; Zhao, Y.; Pelletier, M.; Dan, Y.; Zhao, Y. *Polymer* **2009,** *50,* 3470-3477.

8. Norakankorn, C.; Pan, Q.; Rempel, G. L.; Kiatkamjonwong, S. *European Polymer Journal* **2009,** *45,* 2977-2986.

9. Watnasirichaikul, S.; Davies, N. M.; Rades, T.; Tucker, I.G. *Pharmaceutical Research* **2000,** *6,* 684-689

10. Bisht, S.; Feldmann, G.; Soni, S.; Ravi, R.; Karikar, C.; Maitra, A.; Maitra, A. *J. of Nanobiotech.* ***2007.***

11. An, Z.; Tang, W.; Hawker, C. J.; Stucky, G. D. *J. Am. Chem. Soc.* **2006,** *128,* 15054-15055.

12. Hutchinson, R. A. Free-radical Polymerization: Homogeneous. In *Handbook of Polymer Reaction Engineering;* Meyer, T., Keurentjes, J., Eds.; WILEY-VCH Verlag GmbH & Co. KGaA: Weinheim, Germany, 2005; Vol. 1, pp 153-213.

CHAPTER 4

FUTURE WORK

4.1 Further Functionalization of Nanoparticles

The nanoparticles (NPs) that were synthesized in this work were composed of methyl-methacrylate (MMA), polyethylene-glycol diacrylate (PEG-DA), and acrylic acid (AA). The AA provided a carboxylate functional group on the surface of the NPs; however, other functional groups can be added. For instance, for the binding of NHS-PEG-MAL crosslinker an amine (NH_2) functional group is needed. Therefore, to revisit the coupling of HSA to NPs, NH_2 terminated particles must be synthesized. Due to their therapeutic properties, the binding of transition metals is also being investigated by other members of this research group. Preliminary results indicate that phosphate functionalized NPs bind to a wider selection of transition metals, compared to carboxylate functionalized ones. Thus having different functional groups on the surface of NPs increases their potential uses as drug delivery vectors.

4.2 In vitro Toxicity of Nanoparticles

Before examining the biodistribution of NPs an assay for their toxicity is essential, because if NPs are not biocompatible using them as drug delivery vectors would be more detrimental than beneficial. The in vitro culture of cell lines is the most common assessment for NP toxicity.[1] Major cell types used for

in vitro testing include phagocytic, neural, hepatic, epithelial, endothelial, red blood cells and various cancer cell lines. The specific cell line selected for in vitro assessment is intended to model a response prone to be observed by particles in vivo.[2] Alesha Harris, a member of this group, has received training for testing cytotoxicity of NPs and will be responsible for completing this work before in vivo tests are performed.

4.3 In vivo Biodistribution of Fluorescently-labeled Nanoparticles

Once it is established that the NPs are biocompatible, in vivo tests can be conducted to investigate organ distribution of the fluorescently labeled NPs. To determine the biodistribution of the nanoparticles, fluorescently labeled particles will be administered intravenously to mice. The mice will be injected with 35 µg of the fluorescently labeled acrylate-based NPs. The NP's half-life can be found by drawing 25 µL of blood at certain time points throughout a period of 24 h, and quantifying the number of NPs as a function of time. The mice can then be killed via cervical dislocation, and the brain, heart, kidneys, liver, lungs, and spleen as well as plasma collected. The organs can be analyzed by homogenizing the tissues on ice in 2 mL phosphate-buffered saline, and diluted 100 times. The resulting diluted homogenates can analyzed for fluorescent particles on a plate reader at the appropriate excitation and emission wavelengths.[3,4]

4.4 Biodistribution of Albumin-Coated Nanoparticles

Covalent conjugation of albumin to the surface of NPs via maleimide chemistry proved problematic. Another avenue of research in the Petros lab

involves screening combinatorial peptide libraries for peptide-based ligands that bind to target proteins. Short peptide-based ligands that bind albumin will be elucidated using this methodology, and the effects of those ligands will be examined both in vitro and in vivo.

4.5 Chapter References

1. Jones, C. F., Grainger, D. W., *Adv. Drug Deliv. Rev.,* 2009, *61,* pp. 438-456.

2. Kroll, A.; Pillukat, M. H.; Hahn, D.; Schnekenburger, J. *European Journal of Pharmaceutics and Biopharmaceutics* **2009,** *72,* 370-377.

3. Semete, B.; Booysen, L.; Lemmer, Y.; Kalombo, L.; Katata, L.; Verschoor, J.; Swai, H. S. *Nanomedicine: Nanotechnology, Biology and Medicine, In Press, Corrected Proof.*

4. Merkel, O. M.; Librizzi, D.; Pfestroff, A.; Schurrat, T.; Buyens, K.; Sanders, N. N.; De Smedt, S. C.; Béhé, M.; Kissel, T. *J. Controlled Release* **2009,** *138,* 148-159.

BIBLIOGRAPHY

Aggarwal, P.; Hall, J. B.; McLeland, C. B.; Dobrovolskaia, M. A.; McNeil, S. E. *Adv. Drug Deliv. Rev.* **2009,** *61,* 428-437.

Akagi, T.; Baba, M.; Akashi, M. *Polymer* **2007,** *48,* 6729-6747.

An, Z.; Tang, W.; Hawker, C. J.; Stucky, G. D. *J. Am. Chem. Soc.* **2006,** *128,* 15054-15055.

Bawarski, W. E.; Chidlowsky, E.; Bharali, D. J.; Mousa, S. A. *Nanomedicine: Nanotechnology, Biology and Medicine* **2008,** *4,* 273-282.

Bisht, S.; Feldmann, G.; Soni, S.; Ravi, R.; Karikar, C.; Maitra, A.; Maitra, A. *J. of Nanobiotech.* ***2007.***

Carter, D.C.; Ho, J.X. *Adv. Protein Chem.* **1994,** *45,* 153–203.

Claesson, P.M.; Blomberg,E.; Froberg, J.C.; Nylander, T.; Arnebrant, T. *Adv. Colloid Interface Sci.* **1995,** *57,* 161–227.

Cloninger, M. J. *Curr. Opin. Chem. Biol.* **2002,** *6,* 742-748.

Feng, H.; Zhao, Y.; Pelletier, M.; Dan, Y.; Zhao, Y. *Polymer* **2009,** *50,* 3470-3477.

Francesco, M.V.; Gianfranco, P. *Drug Discov. Today* **2005,** *10,* 1451–1458.

Furumoto, K.; Yokoe, J.; Ogawara, K.; Amano, S.; Takaguchi, M.; Higaki, K.; Kai, T.; Kimura, T. *Int. J. Pharm.* **2007,** *329,* 110-116.

Hamidi, M.; Azadi, A.; Rafiei, P. *Drug Deliv.* **2006,** *13,* 399–409.

Hans, M. L.; Lowman, A. M. *Current Opinion in Solid State and Materials Science* **2002,** *6,* 319-327.

Harper, G.R.; Davies, M.C.; Davis, S.S.; Tadros, T.F.; Taylor, D.C.; Irving, M.P. *Biomaterials* **1991,** *12,* 695–704.

He, Q.; Zhang, J.; Shi, J.; Zhu, Z.; Zhang, L.; Bu, W.; Guo, L.; Chen, Y. *Biomaterials* **2010,** *31,* 1085-1092.

Huang, S. *Adv. Drug Deliv. Rev.* **2008,** *60,* 1167-1176.

Hutchinson, R. A. Free-radical Polymerization: Homogeneous. In *Handbook of Polymer Reaction Engineering;* Meyer, T., Keurentjes, J., Eds.; WILEY-VCH Verlag GmbH & Co. KGaA: Weinheim, Germany, 2005; Vol. 1, pp 153-213.

Jones, C. F., Grainger, D. W., *Adv. Drug Deliv. Rev.,* 2009, *61,* pp. 438-456.

Karmali, P. P.; Kotamraju, V. R.; Kastantin, M.; Black, M.; Missirlis, D.; Tirrell, M.; Ruoslahti, E. *Nanomedicine: Nanotechnology, Biology and Medicine* **2009,** *5,* 73-82.

Koo, O. M.; Rubinstein, I.; Onyuksel, H. *Nanomedicine: Nanotechnology, Biology and Medicine* **2005,** *1,* 193-212.

Kratz, F., *J. Controlled Release* **2008,** *132,* 171-183.

Kratz, F.; Fichtner, I.; Roth, T.; Fiebig, I; Unger, C. *J. Drug Targeting* **2000,** *8,* 305-318.

Kratz, F.; Muller-Driver, R.; Hofmann I.; Drevs, J.; Unger, C. *J. Med. Chem.* **2000,** *43,* 1253-1256.

Kratz, F.; Warnecke, A.; Scheuermann, K.; Stockmar, C.; Schwab, J.; Lazar, P.; Druckes, P.; Esser, N.; Drevs, J.; Rognan, D.; Bissantz, C.; Hinderling, C.; Folkers, G.; Fichtner, I.; Unger,C. *J. Med. Chem.* **2002,** *45,* 5523-5533.

Kroll, A.; Pillukat, M. H.; Hahn, D.; Schnekenburger, J. *European Journal of Pharmaceutics and Biopharmaceutics* **2009,** *72,* 370-377.

Langer, K.; Anhorn, M. G.; Steinhauser, I.; Dreis, S.; Celebi, D.; Schrickel, N.; Faust; S., Vogel, V. *Int. J. Pharm.* **2008,** *347,* 109-117.

Langer, K.; Balthasar, S.; Vogel, V.; Dinauer, N.; von Briesen, H.; Schubert, D. *Int. J. of Pharm.* **2003,** *257,* 169-180.

Liao, L. B.; Zhou, H. Y.; Xiao, X. M. *J. Mol. Struct.* **2005,** *749,* 108-113.

Liu, S.; Wei, X.; Chu, M.; Peng, J.; Xu, Y. *Colloids and Surfaces B: Biointerfaces* **2006,** *51,* 101-106.

Lukyanov, A. N.; Torchilin, V. P. *Adv. Drug Deliv. Rev.* **2004,** *56,* 1273-1289.

Merkel, O. M.; Librizzi, D.; Pfestroff, A.; Schurrat, T.; Buyens, K.; Sanders, N. N.; De Smedt, S. C.; Béhé, M.; Kissel, T. *J. Controlled Release* **2009,** *138,* 148-159.

Microtrac Total Solutions in Particle Size Characterization. http://www.microtrac.com/Home.aspx (accessed May 15, 2010).

Muller, R. H.; Keck, C. M. *J. Biotechnol.* **2004,** *113,* 151-170.

Norakankorn, C.; Pan, Q.; Rempel, G. L.; Kiatkamjonwong, S. *European Polymer Journal* **2009,** *45,* 2977-2986.

Ogawara, K.; Furumoto, K.; Nagayama, S.; Minato, K.; Higaki, K.; Kai, T.; Kimura, T. *J. Controlled Release* **2004,** *100,* 451-455.

Ogawara, K.; Yoshida, M.; Kubo, J.; Nishikawa, M.; Takakura, Y.; Hashida, M.; Higaki, K.; Kimura, T. *J. Control. Release* **1999,** *61,* 241–250.

Owens III,D. E.; Peppas, N. A. *Int. J. Pharm.* **2006,** *307,* 93-102.

Pinto Reis, C.; Neufeld, R. J.; Ribeiro, António J.; Veiga, F. *Nanomedicine: Nanotechnology, Biology and Medicine* **2006,** *2,* 8-21.

Rozenberg, B. A.; Tenne, R. *Progress in Polymer Science* **2008,** *33,* 40-112.

Sahoo, S. K.; Parveen, S.; Panda, J. J. *Nanomedicine: Nanotechnology, Biology and Medicine* **2007,** *3,* 20-31.

Santra, M. K.; Banerjee, A.; Rahaman, O.; Panda, D. *Int. J. Biol. Macromol.* **2005,** *37,* 200-204.

Semete, B.; Booysen, L.; Lemmer, Y.; Kalombo, L.; Katata, L.; Verschoor, J.; Swai, H. S. *Nanomedicine: Nanotechnology, Biology and Medicine, In Press, Corrected Proof.*

Soppimath, K. S.; Aminabhavi, T. M.; Kulkarni, A. R.; Rudzinski, W. E. *J. Controlled Release* **2001,** *70,* 1-20.

Tadros, T.; Izquierdo, P.; Esquena, J.; Solans, C. *Adv. Colloid Interface Sci.* **2004,** *108-109,* 303-318.

Thermo Scientific. http://www.piercenet.com/files/1766dh5.pdf (accessed January, 30, 2009), Instructions for SM(PEG)$_n$ Crosslinkers.

Watnasirichaikul, S.; Davies, N. M.; Rades, T.; Tucker, I.G. *Pharmaceutical Research* **2000,** *6,* 684-689.

Yang, S. C.; Lu, L. F.; Cai, Y.; Zhu, J. B.; Liang, B. W.; Yang, C. Z. *J. Controlled Release* **1999,** *59,* 299-307.

Yokoe, J.; Sakuragi, S.; Yamamoto, K.; Teragaki, T.; Ogawara, K.; Higaki, K.; Katayama, N.; Kai, T.; Sato, M.; Kimura, T. *Int. J. Pharm,* **2008,** *353,* 28-34.

Zhang, J. A.; Anyarambhatla, G.; Ma, L.; Ugwu, S.; Xuan, T.; Sardone, T.; Ahmad, I. *European Journal of Pharmaceutics and Biopharmaceutics* **2005,** *59,* 177-187.